THE ROLE OF PHOSPHODIESTERASES IN CYCLIC NUCLEOTIDE COMPARTMENTATION ACROSS DIFFERENT SIGNALLING PATHWAYS IN THE ADULT RAT VENTRICULAR MYOCYTE

by

Lian Ildiko Szabo

A thesis submitted to the Department of Physiology

In conformity with the requirements for

the degree of Master of Science

Queen's University

Kingston, Ontario, Canada

(July, 2009)

ABSTRACT

In cardiac myocytes, multiple receptor mediated signalling pathways converge on cyclic nucleotide production. These second messengers then act to achieve changes in cellular function. Despite this, each signalling molecule and receptor can achieve distinct sub-cellular effects. This has led to the theory of cyclic nucleotide compartmentation, which has been postulated to be mediated by phosphodiesterases (PDEs). Research in this field has focused on compartmentation using β-adrenergic stimulation. As an extension of this work, we investigated the effects of two agonists, prostaglandin E_2 (PGE_2; 10 nM) and forskolin (FSK; 30 nM), on various cellular parameters in the presence of either cilostamide (1 μM) a selective PDE3 inhibitor, or Ro 20-1724 (10 μM) a selective PDE4 inhibitor. In myocytes treated with PGE_2, unloaded cell shortening and intracellular calcium transients exhibited significantly different ($p<0.05$) values of 147 ± 10% and 138 ± 5% of pre-treatment (t=0) values, respectively, in the presence of both PGE_2 and Ro 20-1724 (all n=5). However, values were not significantly different in cells pre-treated with cilostamide. Conversely, FSK resulted in significant increases of 153 ± 9% (n=5; $P>0.05$) and 189 ± 20% (n=5; $P>0.05$) of t=0 in cells treated with cilostamide and Ro 20-1724, respectively. PGE_2 enhanced $I_{Ca,L}$ was not altered using either PDE inhibitor. However, with FSK as an agonist, a significant increase in peak $I_{Ca,L}$ from -6.0 ± 0.8 pA/pF to -7.7 ± 0.4 pA/pF (n=5; $P>0.05$) was observed in cells pre-treated with Ro 20-1724. SR calcium loading was also increased, but only in cells pre-treated with Ro 20-1724, with values of 127 ± 11% and 156 ± 47% of t=0 (n=5) for FSK and PGE_2, respectively. Our results demonstrate that a unique pattern of regulation exists for PGE_2

and that it is different from what was found previously with isoproterenol. We have shown that this is achieved by functionally localizing PDEs to distinct compartments. Specifically, PDE4 is localized at the SR, PDE3 at the sarcomere, and a combination of both at the calcium channel. However, our $I_{Ca,L}$ results also indicate that the location of the receptor and adenylate cyclases must be considered relevant to compartmentalizing the cAMP signal.

ACKNOWLEDGEMENTS

There are too many people to thank. First of all, I must thank my family. You all helped me in many different ways. Mom and dad, you knew exactly what to say at the right times, even if I didn't always want to hear it. Michael, you kept me younger in a time that was rapidly aging me. Danielle, I could always count on you to distract me from the stress, you always found something that could help me clear my mind. Finally, Chris, you were my pillar that kept me grounded and stable. You helped me put things into perspective, and taught me to never just settle. I couldn't have done this without you here.

I also want to thank everyone in the lab, for you are no longer colleagues but friends as well. Jesse, my teacher, you helped ease me into the research. You gave me a standard that I wanted to live up to. Thank you Jimmy for always bringing a smile to my face, you have such a good heart. I wish you well in your future endeavours. Gina, I want to thank you for the many hours of life talks and the guidance that only your singular position could provide. I also want to thank both the fourth year students, Mike and Christina. It's nice to know that I am always learning, even from those younger than me. Finally, I want to thank you Sarah for saving me in the lab, I'm not sure I could have finished without all your help, encouragement, and support. I know you will be very successful in the future. You are a good person, and a better friend.

I would also like to thank my mentors. Thank you Dr. Fisher, you helped push me beyond my limits and expectations and you showed me the kind of passion that

scientific inquiry can instil. Finally, Dr. Ward, you were the perfect fit for a supervisor, and I'm honoured to have learned so much from you.

As well, I would like to acknowledge the rats that allowed me to complete my research. I will strive to use this knowledge and experience I gained to benefit others.

TABLE OF CONTENTS

LIST OF FIGURES

LIST OF ABBREVIATIONS

AC	Adenylate Cyclase
AKAP	A-kinase Anchoring Protein
AMP	Adenosine Monophosphate
β-AD	β-Adrenergic
β-AR	β-Adrenergic Receptor
cAMP	Cyclic Adenosine Monophosphate
CICR	Calcium Induced Calcium Release
CNG	Cyclic Nucleotide Gated
ECC	Excitation Contraction Coupling
EP-R	Prostanoid Receptor
FRET	Fluorescence Resonance Energy Transfer
FSK	Forskolin
GC	Guanylate Cyclase
GDP	Guanosine Diphosphate
Glu-R	Glucagon Receptor
GPCR	G-Protein Coupled Receptor
GTP	Guanosine Triphosphate
IBMX	Isobutylmethylxanthine
$I_{Ca,L}$	L-Type Calcium Current
ISO	Isoproterenol
K_m	Michaelis Constant

LTCC	L-Type Calcium Channel
MBC-P	Myosin Binding Protein C
mRNA	Messenger Ribonucleic Acid
NCX	Sodium Calcium Exchanger
NO	Nitric Oxide
PDE	Phosphodiesterase
PGE_2	Prostaglandin E_2
PGE_1	Prostaglandin E_1
PKA	Protein Kinase A
PKG	Protein Kinase G
PLB	Phospholamban
RyR	Ryanodine Receptor
SERCA	Sarcoplasmic/Endoplasmic Reticulum Calcium ATP-ase
siRNA	Small Interfering Ribonucleic Acid
SR	Sarcoplasmic Reticulum
TnI	Troponin I
V_{max}	Maximum Velocity

CHAPTER 1: INTRODUCTION & LITERATURE REVIEW

Cell Signalling in the Heart

The mechanisms that allow external stimuli to modify the internal functions of a cardiac myocyte are part of a highly organized and complex signalling system. The activation of a multitude of receptors is what allows a cell to detect changes in the external environment, which ultimately initiates a series of downstream events that facilitate and drive the appropriate response (Reviewed in Wheeler-Jones, 2005). It is therefore of no surprise that this stimulus-response coupling plays a critical role in both physiological and pathophysiological conditions, and is the focus of much scientific debate.

In the heart, function is often affected through modifications to mechanisms involved in excitation-contraction coupling (ECC), the cellular process of converting the electrical stimulus into a mechanical response (Reviewed in Bers, 2008). In response to depolarization, calcium channels open at the junctional cleft, thereby increasing local calcium concentrations. This activates the ryanodine receptors (RyR), which induce calcium release from the sarcosplasmic reticulum (SR) in a process termed calcium-induced calcium-release (CICR). This large rise in calcium in the cleft diffuses towards the contractile apparatus where it binds troponin-C, inducing a conformational change in troponin-I. Consequently, this allows myosin cross-bridge interaction and initiates contraction. As calcium channels close, calcium is sequestered back into the SR by the sarcoplasmic/endoplasmic reticulum calcium ATPase (SERCA), which is normally inhibited by the protein phospholamban (PLB).

One of the primary mediators of ECC modification is the activation of G-protein coupled receptors (GPCRs). In short, GPCR agonists promote the interaction of their respective receptors with a heterotrimer (composed of α, β, and γ subunits). This results in a GTP-GDP exchange on the G_α subunit, causing dissociation. This leaves either the G_α or $G_{\beta\gamma}$ subunits to act on effector molecules, thereby regulating the generation of second messengers. Second messengers are signalling molecules, whose rapid release or synthesis as freely diffusible molecules activates other cellular targets.

Often, multiple signalling pathways will exploit a single second messenger. How very different external stimuli, acting through a common signalling mechanism, are discriminated by the cell to create a unique response is a topic of great interest. In order to understand the theories related to this dilemma, it is first important to address exactly how one of these systems works: the cAMP-PKA signalling axis.

The cAMP-PKA signalling axis

Since its discovery in 1957, cyclic adenosine monophosphate (cAMP) has been shown to play a role as a second messenger in cells throughout the body (Reviewed in Tasken & Aandahl, 2004). Currently, synthesis and degradation pathways of cAMP are known; however, their regulation is less clear (Beavo & Brunton, 2002). In the heart, cAMP activity is related to several diverse functions, ranging from immediate demands for cardiac performance to alterations in gene expression that may ultimately affect structural remodelling, and, therefore, represent an important area of study.

In short, the basic signalling cascade involves GPCR activation, which causes synthesis of cAMP, which acts on its downstream effectors, ultimately altering the activity of a target molecule through phosphorylation. The details of this pathway and how cAMP is regulated within the cell are discussed in the below three sections.

cAMP action: Protein Kinase A (PKA)

In most pathways, cAMP targets protein kinase A (PKA), formerly known as cAMP-dependent protein kinase (Reviewed in Lissandro & Zaccolo, 2006). Since its discovery in the glycogenolysis pathway (Walsh et al, 1968), PKA has been demonstrated to phosphorylate several components involved in ECC, including but not limited to voltage-gated L-type calcium channels (LTCC), RyR (Bers & Perez-Reyes, 1999), troponin I (TnI) (Strang et al, 1994), myosin binding protein C (MBP-C) (Gautel et al, 1995) and phospholamban (PLB) (Hagemann & Xiao, 2002). Consequently, the combined effect of phosphorylating these proteins is generally a combination of positive chronotropy, inotropy and lusitropy. This is achieved primarily by creating an increase in both the peak calcium current ($I_{Ca,L}$) and the amount of calcium released from the SR (Bers & Perez, 1999).

In addition to those effects on excitation contraction coupling mechanisms, cAMP can also target molecules that affect long-term gene expression signalling, such as EPAC, a guanine exchange factor. Its activation through cAMP binding initiates long term changes in cellular structure by initiating downstream effects on gene transcription (Holz et al, 2006). This has been shown to affect such elements as cell adhesion (Rangarajan et

al, 2003) and gap-junction formation (Somekawa et al, 2005). Furthermore, it has been implicated in some pathological conditions, including cardiac hypertrophy (Morel et al, 2005).

Considering the wide role of cAMP signalling, the understanding of its regulation is, therefore, a key factor in determining pathway specificity. Thus, the primary mechanisms of cAMP regulation, synthesis and hydrolysis (degradation), are discussed below.

cAMP synthesis: Adenylate Cyclases (AC)

The synthesis of cAMP from ATP occurs through the common effector molecule adenylate cyclase (AC). There are currently 9 known membrane bound isoforms of ACs (Hanoune & Defer, 2001), with AC5 and AC6 being the most prevalent in the heart (Defur et al, 2000). These transmembrane proteins are stimulated by GPCR action and forskolin, a toxin from *Coleeus forskolii*. It has been proposed that AC5 and AC6 possess distinct roles, however this has yet to be directly demonstrated. For instance, mRNA expression of both isoforms demonstrated a different pattern of downregulation in response to heart failure models (Ping et al, 1997). In addition, differential patterns of expression appear to exist during development (Espinasse et al, 1995).

These findings suggest spatial localization, which would allow the exclusive interaction of cAMP with selective cellular targets, and that subcellular compartments do indeed exist. However, it has been speculated that a localized gradient of cAMP would be impossible through synthesis alone, since the diffusive capacity of cAMP would be

too rapid and widespread. Indeed, it is now agreed that degradation accounts for the total cAMP pool more than its synthesis (Mongillo et al, 2004; Nikolaev et al, 2005), implicating phosphodiesterases (PDEs) as a critical control point for cAMP regulation.

cAMP hydrolysis: Phosphodiesterases (PDEs)

PDEs are the primary mechanisms that limit cAMP levels. These metallophosphohydrolases cleave the 3',5'-cyclic phosphate moiety of cAMP, producing the inert molecule, 5'AMP, thereby rendering it effectively neutral. Currently, there are 11 known PDE families, 5 of which have been shown to be present in the heart (Mongillo & Zaccolo, 2006; Reviewed in Omori & Kotera, 2007).

PDE1 is primarily expressed in non-myocyte cardiac tissue (Bode et al, 1991) and PDE5 is specific to cyclic guanosine monophosphate (cGMP). Consequently, these two families have been shown to contribute very little to cAMP degradation in the ventricular myocyte (Mongillo et al, 2004). Though PDE5 has been shown to be present in the heart on an mRNA (Kotera et al, 1993) and protein level (Senzaki et al, 2001), theories on its direct effects remain inconclusive (Reviewed in Fischmeister et al, 2006).

PDE2, which possesses both cAMP and cGMP hydrolyzing activity, remains quantitatively the least important PDE in the heart (Mongillo et al, 2004). It is activated by the Ca^{2+}/calmodulin complex. Furthermore, it appears to be the only PDE in which intracellular cGMP stimulates its cAMP hydrolyzing capacity (Fischmeister et al, 2005). This is discussed in detail later.

PDE3 and PDE4 combined are responsible for almost 90% of cAMP degradation in cardiac myocytes. PDE3 hydrolyzes both cAMP and cGMP, but due to its higher V_{max} for cAMP, is considered to be cGMP-inhibited. Conversely, PDE4 is cAMP specific, and is thought to contribute to almost twice as much of the hydrolyzing activity in the murine heart than PDE3 (Mongillo et al, 2004).

The specificity of PDE activity indicates that there are limitless applications for pathway regulation. Their role in creating subcellular microdomains has now become the dominant theory in the scientific community and is an active area of research.

Cyclic Nucleotide Compartmentation

Given the tightly regulated synthesis and hydrolysis of cAMP, it is now evident that there exists some manner of spatial-temporal organization, which ultimately could be responsible for the great extent of pathway specificity present in second messenger signalling. Some of the earliest evidence comes from 30 years ago when it was shown that prostaglandin E_1 (PGE_1) and isoproterenol (ISO), a β-AR agonist, created different effects on myocyte contractility, despite both elevating cAMP and PKA activity (Hayes et al, 1979; Corbin et al, 1997). The fact that ISO was capable of inducing positive inotropy, whereas PGE_1 could not, indicated that the increase in cAMP had to occur in a functional microdomain.

Co-localization of receptors with their downstream effectors has been one theory used to explain the formation of functional microdomains. For instance, using immunohistochemistry, it has been shown that β-adrenergic receptors are localized to the

t-tubules, which brings them into proximity with the SR (Orchard & Brett, 2008). Other advances have described the formation of lipid rafts, known as caveolae, which serve as scaffolds that anchor protein complexes together at the sarcolemma (Insel et al, 2005).

Thus, evidence for receptor localization has contributed to the continued growing body of research that is assessing how an uneven distribution of intracellular cAMP is occurring, and what mechanisms may be responsible for this phenomenon (Zaccollo & Posen, 2002; Rich et al, 2001). In addition to the co-localization of the receptors and adenylate cyclases (Rich et al, 2000), others have proposed a form of molecular "channelling" from AC to PKA (Karpen, et al 2000). Both emphasize a role in creating discrete microdomains. However, the former relies on free diffusion of cAMP, whereas the latter suggests barrier molecules that physically delineate the cAMP signal, acting much like a tunnel.

Ultimately however, the theory of compartmentation through PDE activity has gained the most support. The foundations of this theory rely on the notion that PDEs can delineate the boundaries for cAMP diffusion, and create intracellular gradients, thereby allowing modification of defined sets of PKA-mediated intracellular events.

Role of PDEs

The first evidence for the role of PDEs in cAMP compartmentation came from work by on isolated perfused guinea pig hearts (Rapundalo et al, 1989). The authors found that treatments with IBMX (a non-selective PDE inhibitor), milrinone (a PDE3 inhibitor) or isoproterenol, varied in their cellular mechanisms despite a similar increase

in cardiac contractility. Indeed, not only was there a difference in total cAMP, but also in the type and quantity of phosphorylated end-products. Thus, it is now well established that separate pools of particulate and soluble fractions of cAMP activity are responsible for these results, and have been supported on both biochemical (Hohl & Li, 1991) and functional (Jurevicius & Fischmeister, 1996) levels.

It is known that different cellular pathways may involve different PDEs. Nikolaev and colleagues (2006) demonstrated that β_1-AD pathways used primarily PDE4, whereas β_2-AD used multiple PDE types. It is suspected that the ability of PDEs to possess such distinct properties is based on their cellular localization, which ultimately determines their function. The following is a synopsis on the known localization and functions of PDE2, PDE3, and PDE4.

As mentioned previously, PDE2 has a relatively small contribution in the heart. Although it is been shown to be present in the cytosol, it appears to possess a primary role in controlling subsarcollemal concentrations of cAMP. This appears to be due to cross-talk with cGMP. For instance, PDE3 contributes to LTCC regulation when cGMP is increased via local application of NO (Fischmeister et al, 1991). This phenomenon was also observed using FRET-based imaging in β-AD stimulated neonatal rat myocytes (Mongillo et al, 2004).

Conversely, PDE3 appears to be a cGMP-inhibited cAMP hydrolyzing PDE. It is present in both cytosolic and membrane fractions of the cell. However, it has now been demonstrated that specific isoforms of PDE3 are localized, and are associated with independent regulation of cAMP within these compartments (Hayes et al, 1980; Rybin et

al, 2000). This widespread presence may be a reason why competitive inhibitors of PDE3 used for the treatment of heart failure adversely affect long-term survival, and is discussed in the next section.

PDE4 hydrolysis is cAMP specific (Reeves et al, 1987). It has been identified in both the cytosol and membrane fractions of the cell as well, and its isoforms appear to localize differently (Houslay et al, 2007). In cardiac myocytes, PDE4 activity is greatest at the transverse tubule/SR junctional space (Nikolaev et al, 2006). In addition, deficiency in the PDE4D isoform can promote heart failure and exercise-induced arrhythmias. More specifically, the PDE4D3 isoform was associated with changes to RyR modulation caused by excess phosphorylation, creating a 'leaky' SR phenotype (Lehnart et al, 2005). It has also been demonstrated that β-arrestins, an important molecule in inhibiting GPCR activity, recruit PDEs to β-AR. Consequently, local membrane cAMP concentrations may decrease in conjunction with the downregulation of the receptor itself (Perry et al, 2002).

Given the diversity of PDEs and their function, it becomes apparent that research into their roles as therapeutics is a necessity. As such, the following section is devoted to the clinical application of PDE inhibitors.

Clinical Use of PDE Inhibitors

It was first recommended almost two decades ago that PDE3 inhibitors could be used to augment cardiac contractility for the treatment of heart failure (Nicholson et al, 1991). However, it was rapidly demonstrated that chronic treatment with these agents led

to an increase in mortality (Packer et al, 1991). This kind of biphasic response has been shown repeatedly, in which acute treatment can be beneficial by enhancing cardiac function, but chronic administration leads to early mortality (Reviewed in Peronne & Kaplinsky, 2005). It is likely that this is due to the role PDE3 plays in different subcellular compartments.

For instance, the short term hemodynamic benefits are related to the increased phosphorylation of such ECC components as PLB, yielding positive inotropy. However, the widespread presence of PDE3 means that excess phosphorylation of unwanted targets, such as LTCCs, could account for some of the mortality associated with chronic PDE3 use. For example, it has been shown that excess stimulation of the LTCC using isoprenaline can not only prolong action potential duration, but also induce signs of hypertrophy (Meszaros et al, 1997), both of which can contribute to heart failure and cardiac arrest.

Another mechanism for the adverse long-term effects is by affecting its role as an antiapoptotic agent. It has been noted that during heart failure, PDE3 is downregulated (Smith et al, 1998). Associated with this is the induction of inducible cAMP early repressor (ICER) (Ding et al, 2005), which represses antiapoptotic agents in a positive feedback fashion.

The non-specific targeting of PDE3s is most likely responsible for the increased mortality related to chronic PDE inhibition. The fact that specific isoforms are localized may present novel pharmacological targets that could exploit only certain components, and indeed this is now an active area of research.

A-Kinase Anchoring Proteins (AKAPs)

It has also been proposed that the specificity of a cAMP signal is reinforced by scaffolding proteins that tether complexes of receptors, effectors, modulators, and targets all together in a localized microdomain. As a consequence, the probability of cAMP interacting efficiently is greatly increased. More specifically is the importance of sequestering PKA through A-kinase anchoring proteins (AKAPs). These proteins possess an amphipathic helix that can preferentially bind the N-terminal domain of the RII homodimer of PKA (Carr et al, 1992; Alto et al, 2003). Consequently, RII subunits are more prevalent in particulate fractions, whereas RI subunits are dominant in the soluble fractions (Scott, 1993).

Understanding of how AKAP-PKA interactions occur was furthered by the discovery of human thyroid AKAP Ht31 (Ht31 peptide). Ht31 competes for the binding position of RII, and has been shown in cardiac myocytes to disrupt the binding of PKA to AKAPS, specifically blocking phosphorylation of TnI and MBP-C, but not PBL (Fink et al, 2001). This selectivity is a clear indication that physical localization contributes to the compartmentation of cAMP. Several AKAPs have been identified in the heart, though many remain unidentified (Reviewed in Scott, 2006).

Crosstalk: The combined effect of cGMP and cAMP

Cardiac function is also regulated through cGMP pathways. In summary, the activation of guanalyate cyclases (GC), by either NO or natriuretic peptides, causes rapid

synthesis of cGMP. As a consequence of its release, negative inotropic and metabolic effects occur through its effectors protein kinase G (PKG) and CNG channels (Shah & MacCarthy, 2000). cAMP and cGMP pathways are thought to have opposing effects, which is generally attributed to the opposing effects of their effectors. However, it's becoming apparent that they do interact at an earlier stage of signalling. In particular, cAMP concentration can be affected by cGMP sensitive PDEs (Zaccolo & Movsesian, 2007).

As discussed prior, several cAMP-hydrolyzing PDES differ in their affinity and specificity for both cAMP and cGMP. Of the PDEs present in the heart, PDE1, PDE2, PDE3 and PDE5 all possess the capacity to affect cAMP concentration by restricting diffusion. This can occur in two ways: cGMP-stimulated cAMP-PDE activity and cGMP-inhibited cAMP-PDE activity.

PDE2 has uniquely been identified as a cAMP-hydrolyzing PDE that is stimulated by cGMP. It can hydrolyze both cAMP and cGMP, with K_m values of 30 μmol/L for cAMP and 10 μmol/L for cGMP (Martins et al, 1982). cGMP can also bind to a GAF domain on PDE2, which through allosteric modifications, lowering its K_m for cAMP, effectively stimulating cAMP hydrolysis (Martinez et al, 2002).

This phenomenon may possess physiological consequences. For instance, β-AD stimulation of cAMP production is reduced in response to sodium nitroprusside, a NO donor which increases cGMP production (Mongillo et al, 2006). In fact, this phenomenon was selective as well, where rises in cGMP failed to elicit PDE2 cAMP hydrolysis when stimulated with forskolin.

This blunted response to β-AD stimulation may provide a protective effect against excessive pathway activation. Alternatively, it's been postulated that it may decrease the sympathetic reserve in failing hearts, during which β-AR are downregulated (Brodde, 1993). In either case, it is unclear exactly how this cGMP mediates the hydrolysis of cAMP. On the other hand, the higher catalytic rate of PDE3 for cAMP rather than for cGMP, make PDE3 a cGMP-inhibited cAMP-hydrolyzing PDE. This inhibitory phenomenon has been demonstrated both in vitro and in vivo. For instance, LTCCs are potentiated by inhibited PDE3 activity upon GC stimulation in frog ventricular myocytes (Frace et al, 1993).

Similarly, PDE1 may also be inhibited by cGMP activity, however its relevance to cardiac contractility is unresolved (Bode et al, 1991), despite its abundance in the heart (Hambleton et al, 2005). Furthermore, studying its effects has been limited by lack of specific inhibitors for PDE1 (Zaccolo & Movsesian, 2007).

The combined effects of two second messengers on signalling, indicates that a high degree of regulation must occur in both cases. Indeed, there is evidence that cGMP concentrations are controlled as tightly as cAMP. This is supported by the fact that specific concentration ranges of cGMP dictate how it exerts its effects. For example, in human atrial cells, low concentrations of cGMP stimulate I_{Ca}, whereas high concentrations inhibited I_{Ca} (Mery et al, 1993). More direct evidence regarding exact concentration-responses on specific PDE activity remains unknown.

Finally, it is now widely recognized that cGMP is compartmentalized as evidenced its non-uniform cellular distribution. This is likely attributed to the subcellular

localization of soluble and particulate GCs and PDE5 (Reviewed in Castro et al, 2006). Consequently, independent pools of cGMP could affect select pools of cAMP, making a highly selective regulatory mechanism in signalling.

Conceptual Models of Compartmentation

Until recently, the theories regarding how compartmentation is achieved adhered to a "barrier hypothesis" of PDE activity (Rich et al, 2000). In this scenario, tethered PDEs create a wall-like barrier to cAMP, thereby restricting its diffusion from specified microenvironments. What limits the application of this theory is that intracellular cAMP would uniformly decrease in concentration as it got further from its site of production. Consequently, activation of PKA within the deep cytosol would necessitate the concurrent activation of PKA localized at the plasma membrane.

An alternate theory, the "sink hypothesis", is based on the notion that cAMP can diffuse at an effective concentration throughout the entirety of a cell (Reviewed in Zacollo, 2006). Therefore, to restrict its activity, PDEs act as sinks to prevent inappropriate activation of PKAs within specified microdomains. Consequently, multiple domains with varying concentrations of cAMP may exist simultaneously within the cell.

Compartmentation Across Pathway Activation

Much of the research regarding PDE compartmentation has been done using β-AD agonists, whereas other pathways of activation have been less explored. Nonetheless, it is likely that the specificity of the cAMP signal from different GPCR

agonists is created by a distinct pattern of PDE activity. In a study by Rochais and colleagues (2006) recombinant cyclic-nucleotide gated channels (CNG) were used as a cAMP biosensor. These authors found that specific subsets of PDEs are functionally localized to the LTCC and are coupled to specific GPCRs. For instance, Glucagon-receptor (Glu-R) cAMP activity was entirely regulated by PDE4; whereas, β_2-AD cAMP was mediated by both PDE3 and PDE4 activity.

However, there is still little research regarding how these differences in cAMP affect other components of ECC. Furthermore, it has yet to be shown how the combined effects of different PDEs in various pathways affect the functional outcome of cardiac contractility. Preliminary work in our lab has defined the roles of PDE3 and PDE4 as mediators of the β_2-AD signalling pathway. We have found that both PDE3 and PDE4 occupy select subcellular compartments where they limit the actions of increased cAMP concentrations following β_2-AD stimulation. For instance, PDE4 appeared to play a greater role in LTCC regulation, whereas PDE3 is perhaps localized more at the contractile apparatus, which was demonstrated by its greater contribution to cell contractility. However, we now wish to extend these studies to examine the effects of other stimulators of the cAMP pathway to investigate how PDE compartmentation plays a role in determining the cellular actions of such agonists.

Hypothesis and Objectives

The preceding discussion demonstrates that receptor specificity may play a role in creating distinct cellular responses. In an effort to further explore this issue, we will examine multiple pathways, forskolin (FSK; a direct adenylate cyclase activator), Prostaglandin E_2 (PGE_2) and Prostaglandin E_1 (PGE_1), both EP receptor agonists. Specifically, we wish to assess how selective PDE3 and PDE4 inhibition combined with one of these agonists will affect specific ECC mechanisms. For these studies, **we hypothesize that the compartmentation created by PDEs will be the determining factor in mediating the distinct cellular actions of agonists that increase cAMP.** Further, we suspect that there may be different cellular effects on our measures of cell function depending on agonist used, ultimately reflecting a combination of both receptor and PDE compartmentation.

To test this hypothesis, we used freshly dissociated right ventricular myocytes from adult male Sprague Dawley rats. Using this model, we characterized how various ECC mechanisms responded to agonist enhanced PDE inhibition. Specifically, we used unloaded cell shortening as an overall indication of contractility. Fluorescence techniques were used to assess intracellular calcium transients and SR loading. Finally, patch clamp experiments, using the perforated-patch configuration, assessed modulation of cellular electrophysiology (including action potentials and their underlying ionic currents). Thus, our specific objectives included the following:

1. Determine concentrations for PGE_2 and FSK to be used in PDE inhibition studies. The concentrations should cause significant but minimal increases in

cell shortening to allow for a full range of measurement if increases in function are present.

2. Examine the combined effects of PGE_2 or FSK and selective PDE inhibitors on unloaded cell shortening, calcium transients, SR calcium loading and the L-type calcium channel.
3. Determine if there are effects on potassium currents and action potential duration when treated with FSK and PDE inhibitors.

CHAPTER 2: METHODS

Isolation of Right Ventricular Myocytes

In accordance with a protocol approved by the Queen's University Animal Care Committee based on the Canadian Council Animal Care Guidelines, male Sprague Dawley rats (~5 weeks old) were killed through decapitation, and the heart was excised and placed on a standard Langendorff apparatus. The heart was then retrogradely perfused at ~10mL/min via the aorta using the following protocol. All solutions were kept at 37±1 °C and continuously gassed with 100% O_2:

1. 5 min of Tyrode's solution containing (in mM): NaCl 140; KCl 5.4; $MgCl_2$ 1; Na_2HPO_4 1; HEPES 5; glucose 10; $CaCl_2$ 1; pH adjusted to 7.4 with NaOH
2. 5 min of calcium-free Tyrode's
3. 7 min of modified Tyrode's (50 µM of $CaCl_2$) containing collagenase (0.02 mg/mL, Type II, Yakult Co. Ltd, Tokyo) and protease (0.004 g/250 mL, Type XIV, Sigma)

Following this, the right ventricular wall was dissected and minced for further digestion in 10mL of Tyrode's solution containing collagenase (0.5 mg/mL, Type II, Yakult Co, Ltd. Tokyo), protease (0.1 mg/mL, Sigma), bovine serum albumin (2.5 mg/mL, Sigma), and $CaCl_2$ (50 µM). This solution was agitated in a bath maintained at 37°C, and was monitored for dissociated cells. Once observed, cells were placed into 3mL aliquots of KB storage solution containing (in mM): potassium glutamate 100; potassium aspartate 10; KCl 25; glucose 20; KH_2PO_4 10; Hepes 5; $MgSO_4$ 2; taurine 20; creatine 5; and EGTA 0.5; 1 mg/mL BSA; pH adjusted to 7.2 with KOH. Aliquots were

taken every 3 min for a total digestion time of ~40 min. Myocytes were stored in KB solution at 4 °C until needed.

Cell Shortening Measurements

Cells were placed in the perfusion chamber on the stage of an inverted microscope (Nikon TE2000) and allowed to adhere to the glass bottom for 10 min. Subsequently, superfusion of the myocytes with Tyrode's solution was maintained at a flow rate of 2 mL/min using a gravity feed system. Myocytes were electrically stimulated by a Grass (SD9) field stimulator (20-40 mV) at a frequency of 1Hz. Cell shortening was measured by a video image feed linked to an edge detection device (Crescent Electronics, USA). This signal was converted and analyzed using pClamp 9.0 / Digidata 1320 data acquisition system.

Since a large drop in contractility occurs from the onset of stimulation, cells were given 5 min to stabilize prior to any drug application. Shortening data were expressed as fractional values (percent change in cell length), which was then normalized for the value at t=0, since this allowed us to measure the response at the onset of the cAMP agonist.

Electrophysiological Methods

Perforated patch-clamp methods were used to record calcium and potassium currents, and action potentials. All experiments were done at room temperature (21-22 °C), and all data was acquired and analyzed using pClamp 9.0 or higher/Digidata 1320 data acquisition system.

Potassium Current and Action Potential Recordings

Cells were plated in the perfusion chamber of an inverted microscope (Nikon TE2000) and superfused with Tyrode's solution using a gravity fed flow system (2mL/min). Fire-polished borosilicate glass pipettes (WPI, Sarasota, FL, USA) were prepared using a microprocessor-controlled, multiple stage puller (model P97, Sutter Instruments). Resistances fell within a range of 1-2 MΩ when filled with the following internal solution (mM): KCl 20; K-Aspartate 110, EGTA 10, HEPES 10, $MgCl_2$ 1, K_2ATP 5, $CaCl_2$ 1, NaCl 10; pH adjusted to 7.2 with KOH. This solution created a liquid junction potential of 10 mV which was corrected for offline.

For perforated patch, an amphotericin stock (Sigma) was prepared at ~1 mg/10µL of DMSO. Prior to experiments, 3.33 µL of stock was sonicated with 1 mL of internal solution, and would remain stable for up to 2 hrs if kept protected from UV light. Before back-filling, pipette tips would be dipped in amphotericin-free internal solution to improve sealing.

Cardiac myocytes were selected primarily based on visual assessment. Overall cell health was indicated by smooth edges, clear and organized striations, and a retained rectangular shape.

Potassium Current Voltage-clamp protocols and Analysis

Whole-cell current and voltage clamp data were collected using a patch-clamp amplifier (Axopatch-1D, Axon Instruments). Currents were sampled at 10 KHz and

filtered at 1 KHz. All current magnitudes were normalized to cell capacitance. Capacitative currents were elicited using 30 msec, +5 mV depolarizing pulses from a holding potential of -80 mV. Capacitance and series resistance were calculated immediately prior to beginning each experiment, as well as at the end of each experiment. For experiments in which there was a discrepancy in capacitance values greater than 10% throughout the experiment, the data were discarded.

Potassium current-voltage relationships were elicited by using a series of square waveforms (using a range of pulses from -120 to +50 mV), with and without a prepulse (a depolarizing step of -40 mV for 100 msec). The transient outward current (I_{to}) was isolated by subtracting the prepulse tracing from the total potassium tracing, since the prepulse inactivates the voltage dependent I_{to}. The sustained outward (I_{sus}) and potassium inward (I_{K1}) currents were analyzed using the prepulse recordings, since these were absent of I_{to}. It is understood that I_{K1} is activated within a lower voltage range (-120 to -60 mV), whereas I_{sus} is activated at more positive voltages (-50 to +50 mV). We therefore deemed it reasonable to not use $BaCl_2$ to selectively block I_{K1}, since it is possible to assess the current voltage-relationship of these two currents over specified voltage ranges.

Action Potential protocols and Analysis

Action potentials were recorded under the same recording conditions as potassium currents. Under current clamp conditions, action potentials were elicited by a brief (5

msec) current injection (700 pA). Action potential waveforms were analyzed offline to assess APD90.

Calcium Current Recordings

Calcium currents were recorded using a modified Tyrode's solution containing (in mM): NaCl 140; CsCl 3; $CaCl_2$ 1; KCl 5.4, Na_2HPO_4 1; HEPES 5; glucose 10; $MgCl_2$ 1; Lidocaine 0.25; pH adjust to 7.4 with NaOH. Also, an alternate internal solution was used, which contained (in mM): CsOH 120; aspartic acid 120; CsCl 30; $MgCl_2$ 1; Na_2ATP 5; HEPES 10; EGTA 1; pH adjusted to 7.2 with CsOH. L-type Ca^{2+} currents were elicited using a 300 ms depolarizing pulse to 0 mV from a holding potential of -40 mV. This step depolarization was preceded by a 1 second ramp from -80 mV to -40 mV to voltage inactivate sodium. The current-voltage relationship was assessed using a square waveform voltage-step protocol (-120 mV to +60 mV) starting from a holding potential of -80 mV.

Intracellular calcium transients

For fluorescent determination of relative intracellular calcium concentrations, myocytes were incubated for 30 min with Fluo3-AM (2.28 µM; Invitrogen/Molecular Probes, Carlsbad, CA).

Cells were continuously superfused with Tyrode's solution, and all experiments were done at room temperature (21-22 °C). Cells were visualized using a 100X objective (Nikon) with Type A immersion oil.

The Fluo-3AM was excited using a wavelength of 480 nM using a high speed multi-wavelength illuminator (DX-100 optical switch; Solamere Tech Group). Fluorescence emission was monitored at 510 nm using a microfluorimeter (SFX2, Solamere Tech Group) and digitized using pClamp 9.0 or higher/Digidata 1320 data acquisition systems.

Cells were field stimulated at a frequency of 1Hz to elicit calcium transients. Immediately prior to caffeine application, the stimulator was turned off. A rapid solution exchanger was used to briefly expose the myocytes to 50 mM caffeine. The resultant changes of fluorescence were recorded for later analysis. The stimulator was then turned on and the cell washed with Tyrode's for 5 min, and allowed to re-stabilize prior to further drug application.

Changes in intracellular calcium (calcium transients) were calculated by expressing the peak fluorescence intensity (F) as a fraction of its baseline (F_0). This ratio was then expressed as a percent fluorescence of the value at t=0 (time prior to cAMP agonist application). The SR load was calculated by integrating the curve, thereby giving a measure of total calcium release. This was expressed as a percent of the value at t=0 to yield a percent fluorescence.

Drug Preparation and Application

For shortening, calcium imaging, SR loading, and patch-clamp experiments, drugs were applied via addition to the bath perfusion system. No more than 5 µL/50 mL

of stock solution was used in order to avoid side-effects from vehicles (either DMSO or ethanol).

Drugs were prepared as follows:

- Forskolin (30 nM, Sigma), DMSO solvent
- Isoproterenol (10 nM, Sigma), H_20_{dd} solvent
- PGE_2 (100 nM, Sigma), ethanol solvent
- Cilostamide (1 µM, Sigma) DMSO solvent
- Ro 20-1724 (10 µM, Calbiochem) DMSO solvent

For all experiments, baseline levels were recorded before and after 2-5 min of stabilization. PDE inhibitors were then applied for a minimum of 5 min, and then cAMP agonists with PDE inhibition for 15 min. A schematic of this protocol is shown in Figure 1.

Study Limitations

For the most part we attempted to minimize the known sources of error. We used freshly isolated ventricular cells that were used within 6 hours of collection, since experience has shown that electrophysiological parameters significantly deteriorate following storage over 8 hours. In addition, we kept our pharmacological agents fresh, particularly the more unstable compounds like PGE_2. These were refreshed every 3 months.

Furthermore, we noticed a significant amount of cell deterioration during cell shortening and fluorescent imaging experiments, and proposed that this could have been due to free radical production from the field stimulator electrodes. As a result, we

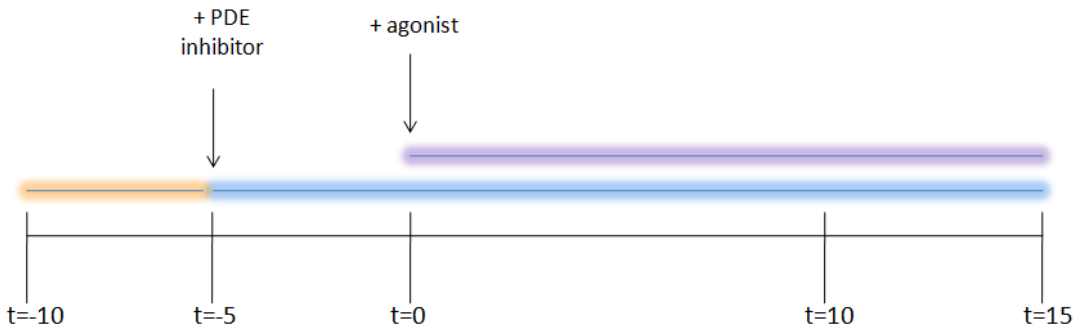

Figure 1. Schematic of drug application protocol. Experiments began with a stabilization period of five minutes. Following this, PDE inhibitors were pre-treated, if required, for the following five minutes. Then, at t=0, the agonist (either FSK or PGE_2) was added to the superfusion solution. Recordings were then made every two minutes for ten minutes, and once again at fifteen minutes.

maintained a flow rate of 2 mL/min, which helped to reduce cell death. Also, we designed exclusion criteria to ensure cell viability. This was primarily based on visual assessment, with a selection for cells with clean borders and clear striations. However, we would also reject cells that exhibited spontaneous contractions, unusual tracings in the SR transient, and if alterations in perfusion rate occurred.

Statistical Analysis

Results are expressed as mean ± standard error of the mean (SEM). Statistical analyses and tests were done using GraphPad Prism 4.0 or greater software. Unpaired student t-tests were used to compare two value data sets. When comparing three or more experimental groups, statistical analysis was done using the Kruskal-Wallis (non-parametric ANOVA) test followed by post-hoc analysis (Dunns test) where appropriate. Statistical significance was given if p-values <0.05.

CHAPTER 3: PROSTAGLANDIN RESULTS

Receptor Mediated Agonists – Prostaglandins (PGE_2 and PGE_1)

Prostaglandin concentration-response curve

Prior to investigating the combined effects of PDE inhibitors and PGE_2, it was necessary to determine a concentration that resulted in a modest increase in contractile function. The rationale for this is that, as we predict that PDE inhibitors will potentiate the effects of PGE_2 on cellular function, minimal stimulation allows a greater range within which the full effects of the PDE inhibitors could be quantified. To determine unloaded cell shortening, right ventricular myocytes were continuously superfused with Tyrode's solution and field stimulated at 1Hz. Various concentrations of PGE_2 were then added to the superfusion solution and unloaded cell shortening was recorded every two minutes for a period of ten minutes and then once again at 15 minutes (Figure 2A).

Following 10 minutes superfusion, the vehicle control group decreased to 76 ± 8% (n=5) of pre-treatment (t=0 min) values. In contrast, 10 minutes of superfusion with 10 nM PGE_2 increased unloaded cell shortening to 110 ± 10% (n=5) of pre-treatment values. At 100 nM PGE_2, an increase of unloaded cell shortening of 136 ± 15% (n=5), relative to t=0, was observed. However, further increasing the PGE_2 concentration to 1 μM resulted in shortening values of 133 ± 23% (n=5) of t=0, which were not increased beyond those observed at 100 nM. Representative traces are shown in Figure 2C.

There was no evidence of calcium overload at any concentration, suggesting that PGE_2 is unable to maximally stimulate the cAMP signalling pathway on its own.

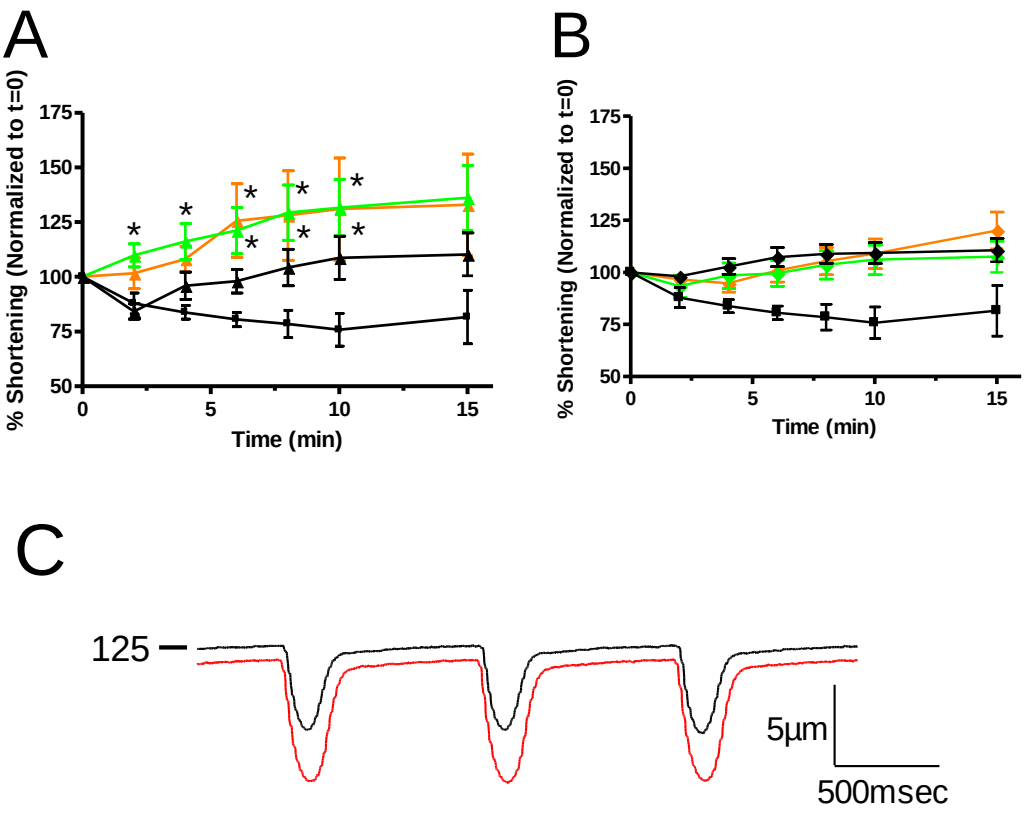

Figure 2. Concentration-Dependent Effects of Receptor Mediated Agonists on Cell Shortening. Ventricular myocytes were superfused with Tyrode's solution and continuously field stimulated at 1Hz. They were then treated with various concentrations of PGE_2 (Panel A): vehicle (■); 10 nM (▲); 100 nM (▲) and 1 µM (▲), or various concentrations of PGE_1 (Panel B): vehicle (■); 10 nM (◆); 100 nM (◆) and 1 µM (◆). Data are expressed as a percentage of unloaded cell shortening relative to t=0, the time at which the agonist was added to the superfusion solution. Values represent the mean ± SEM for n=5 experiments. (*) indicates data that is significantly different ($p<0.05$) from vehicle. Panel C: Representative data illustratingthe effects of 100 nM PGE_2 on unloaded cell shortening. Sample tracings were recorded at t=0 (black) and t=15 (red). Diastolic cell lengths (µm) are listed above baseline region in sample traces.

Thus, we decided to use 10 nM PGE_2 for our remaining experiments, as this concentration elicited insignificant sub-maximal stimulation with minor increases in cell shortening. This would ensure that any potentiated effects from PDE inhibition could be measured to its fullest extent.

In addition to PGE_2 we used PGE_1 as an analogous receptor mediated agonist. Using the same protocol as above, we treated right ventricular myocytes with various concentrations of PGE_1 while field stimulating at 1Hz (Figure 2B). 10 nM, 100 nM and 1 µM all led to similar effects on unloaded cell shortening, with percent shortening values of 110 ± 6%, 108 ± 7%, and 120 ± 9%, of t=0, respectively (all n=5). None of these were significantly different. Thus, there was no observed concentration-dependent effect of PGE_1 on unloaded cell shortening.

Effects of PDE inhibitors on prostaglandin enhanced cell shortening

To evaluate the role of PDEs on unloaded cell shortening, we began by assessing their contributions using two PDE inhibitors, cilostamide (1 µM; Sigma), selective for PDE3, and Ro 20-1724 (10 µM; Calbiochem), selective for PDE4. Drug application followed the protocol discussed above in the Methods section (figure 1), and was used for all the following PDE inhibition experiments.

As seen in Figure 3, following pre-treatment with Ro 20-1724, 10 minutes superfusion with 10 nM PGE_2 significantly increased unloaded cell shortening to 147 ± 10% (n=5) of t=0 values, which was significantly greater than 10 nM PGE_2 alone (110 ± 10%; n=5). In contrast, for myocytes pre-treated with cilostamide, PGE_2 exposure only

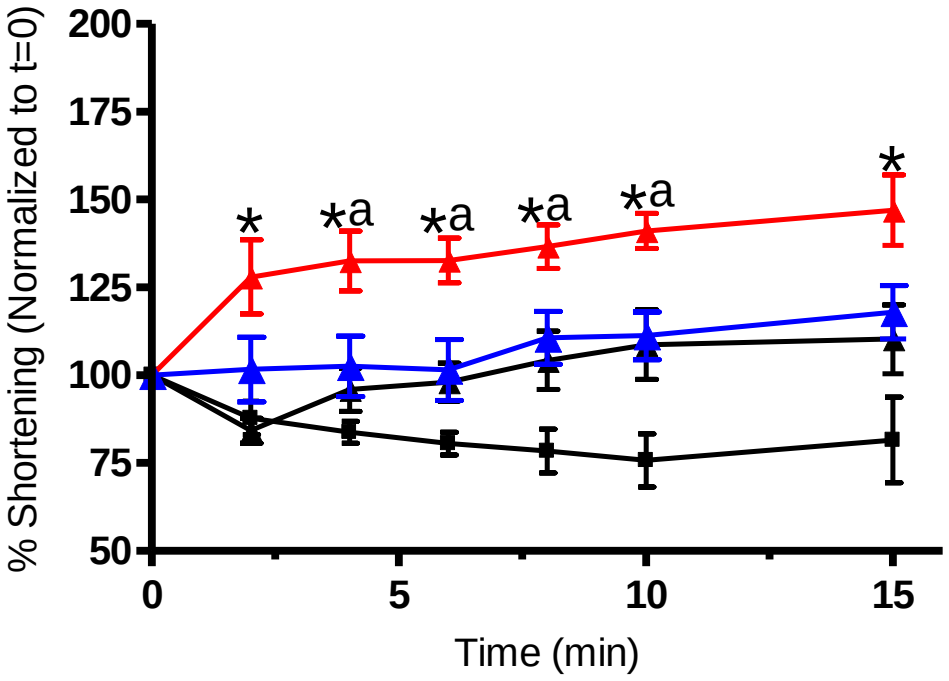

Figure 3. The Effects of PDE Inhibition on Prostaglandin E_2 (PGE_2) Enhanced Cell Shortening. Ventricular myocytes were superfused with Tyrode's and continuously field stimulated at 1 Hz. The effects of vehicle (■), PGE_2 (10 nM; ▲), PGE_2 and cilostamide (10 nM and 1 µM, respectively; ▲), and PGE_2 and Ro 20-1724 (10 nM and 10 µM, respectively; ▲) are shown. Data are expressed as a percentage of unloaded cell shortening relative to t=0, the time at which PGE_2 was added to the superfusion solution. Values represent the mean ± SEM for n=5 experiments. (*) indicates values that are significantly different ($p<0.05$) from 10 nM PGE_2, and (a) indicates those values significantly different ($p<0.05$) from PGE_2 and cilostamide data.

increased unloaded cell shortening to 118 ± 8% (n=5) of t=0 values, which was not significantly different from 10 nM PGE_2 alone. In neither experimental group was calcium overload evident with these treatments.

A similar pattern of responses was observed when PGE_1 was used as the agonist (Figure 4). 10 minutes superfusion with PGE_1 in myocytes pre-treated with Ro 20-1724, resulted in unloaded cell shortening of 157 ± 15% (n=5) of t=0 values. For experiments in which myocytes were pre-treated with cilostamide, unloaded cell shortening values were 129 ± 12% (n=5) of t=0 values.

Combined Effects of PDE Inhibitors and Prostaglandins on Intracellular Calcium Transients

Intracellular calcium transients were recorded to determine the effects of PDE inhibitors on agonist-induced increases of intracellular calcium concentrations. These experiments were conducted in myocytes incubated with Fluo-3AM, a calcium-sensitive dye. Cardiac myocytes were field stimulated at 1 Hz and drugs were added at the same time intervals indicated in the unloaded cell shortening experiments.

Calcium transient results using PGE_2 were very similar to those observed for unloaded cell shortening (Figure 5A). Under conditions in which no PDE inhibitors were used, 10 nM PGE_2 increased peak calcium transients to 113 ± 7% (n=5) of t=0 values. In myocytes pre-treated with cilostamide (1μM), 10 minutes superfusion with 10 nM PGE_2 increased calcium transient amplitudes to 118 ± 6% (n=5) of t=0 values. In contrast, pre-treatment with Ro 20-1724 (10 μM), 10 minutes superfusion with PGE_2 increased

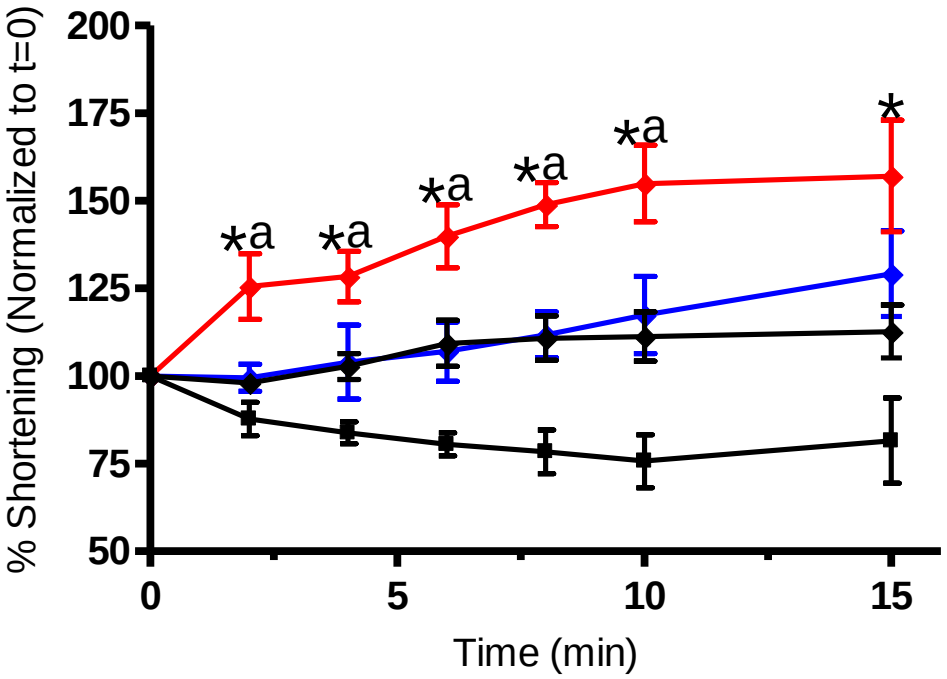

Figure 4. The Effects of PDE Inhibition on Prostaglandin E_1 (PGE_1) Enhanced Cell Shortening. Ventricular myocytes were superfused with Tyrode's and continuously field stimulated at 1Hz. The effects of vehicle (■), PGE_1 (10 nM; ◆), PGE_1 and cilostamide (10 nM and 1 µM, respectively; ◆), and PGE_1 and Ro 20-1724 (10 nM and 10 µM, respectively; ◆) are shown. Data are expressed as a percentage of unloaded cell shortening relative to t=0, the time at which PGE_1 was added to the superfusion solution. Values represent the mean ± SEM for n=5 experiments. (*) indicates those values that are significantly different ($p<0.05$) from 10 nM PGE_1 data, and (a) indicates those that are significantly different ($p<0.05$) than the combined PGE_1 and cilostamide group.

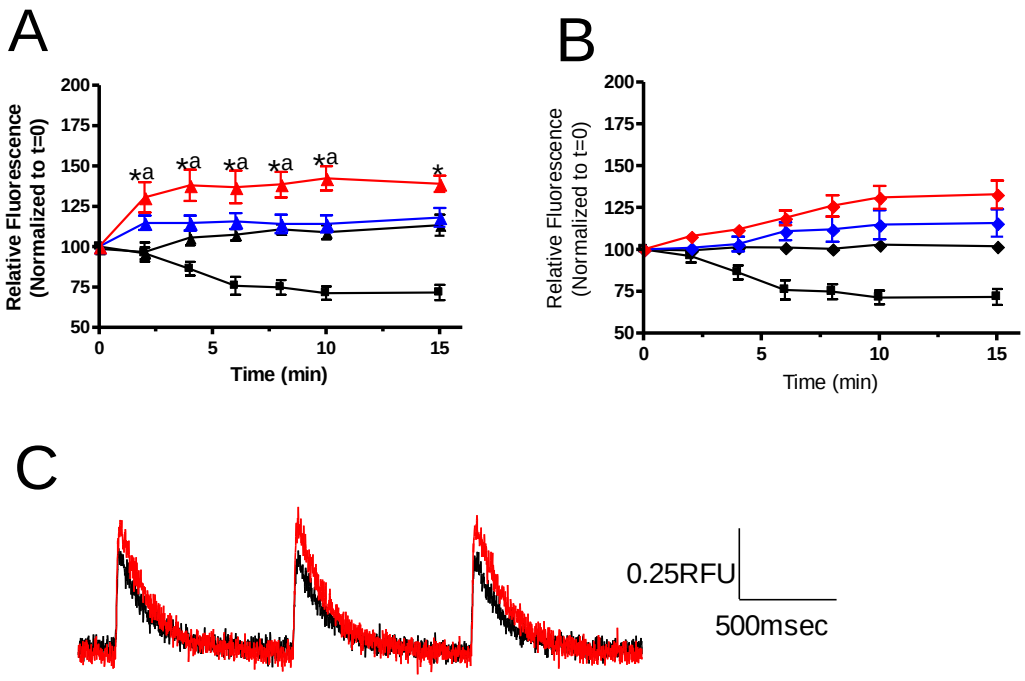

Figure 5. The Effects of PDE Inhibition and Receptor Mediated Agonists on Intracellular Calcium Transients. Ventricular myocytes were superfused with Tyrode's solution and continuously field stimulated at 1 Hz. Panel A: Effects of vehicle (■), PGE_2 (10 nM; ▲), PGE_2 and cilostamide (10 nM and 1 µM respectively; ▲), and PGE_2 and Ro 20-1724 (10 nM and 10 µM respectively; ▲). Panel B: Effects of vehicle (■), PGE_1 (10 nM), PGE_1 and cilostamide (10 nM and 1 µM respectively; ◆), and PGE_1 and Ro 20-1724 (10 nM and 10 µM respectively; ◆). Data are expressed as a percentage of peak calcium transient relative to t=0, the time at which the agonist was added to the superfusion solution. Values represent the mean ± SEM for n=5 experiments. (*) indicates data that is significantly different ($p<0.05$) from 10 nM PGE_2, and (a) indicates those that are significantly different ($p<0.05$) than the combined PGE_2 and cilostamide data. Panel C: Representative data illustrating the effects of Ro 20-1724 pre-PGE_2 (black) and post-PGE_2 (red) at t=15 on intracellular calcium transients. Units are expressed in relative fluorescence units (RFU).

calcium transient amplitudes to 138 ± 5% (n=5) of t=0 values, which is significantly different from the PGE_2 treatment alone. Representative data is shown below (Figure 5C)

The same experiments were also repeated using PGE_1 as the agonist (Figure 5B). PGE_1 increased peak calcium transients to 112 ± 7% (n=5) of t=0 values. Cilostamide and Ro 20-1724 led to further increases in peak transients, with values of 129 ± 12% (n=5) and 157 ± 16% (n=5) of t=0, respectively. However, these data were not significantly different from control.

Effects of PDE Inhibition and PGE_2 on SR Loading

A caffeine pulse protocol using fluorescent imaging allowed a relative measurement of calcium load in the SR. Cells were pre-incubated with Fluo3-AM, and then superfused with Tyrode's solution to remove extracellular dye. The rapid application of caffeine (100 mM; Sigma) causes a sudden increase, followed by a gradual decrease in fluorescence intensity, which we define as a caffeine transient. The amount of calcium stored in the SR is proportional to this caffeine transient and is quantified by determining the area under the curve. Representative tracings of caffeine transients are illustrated in Figure 6B. A percent difference of before (t=0) and after (t=10) PGE_2 application was calculated and graphed (Figure 6A). 10 nM PGE_2 increased SR load yielding a percent change of 130 ± 14% (n=5) from t=0 values

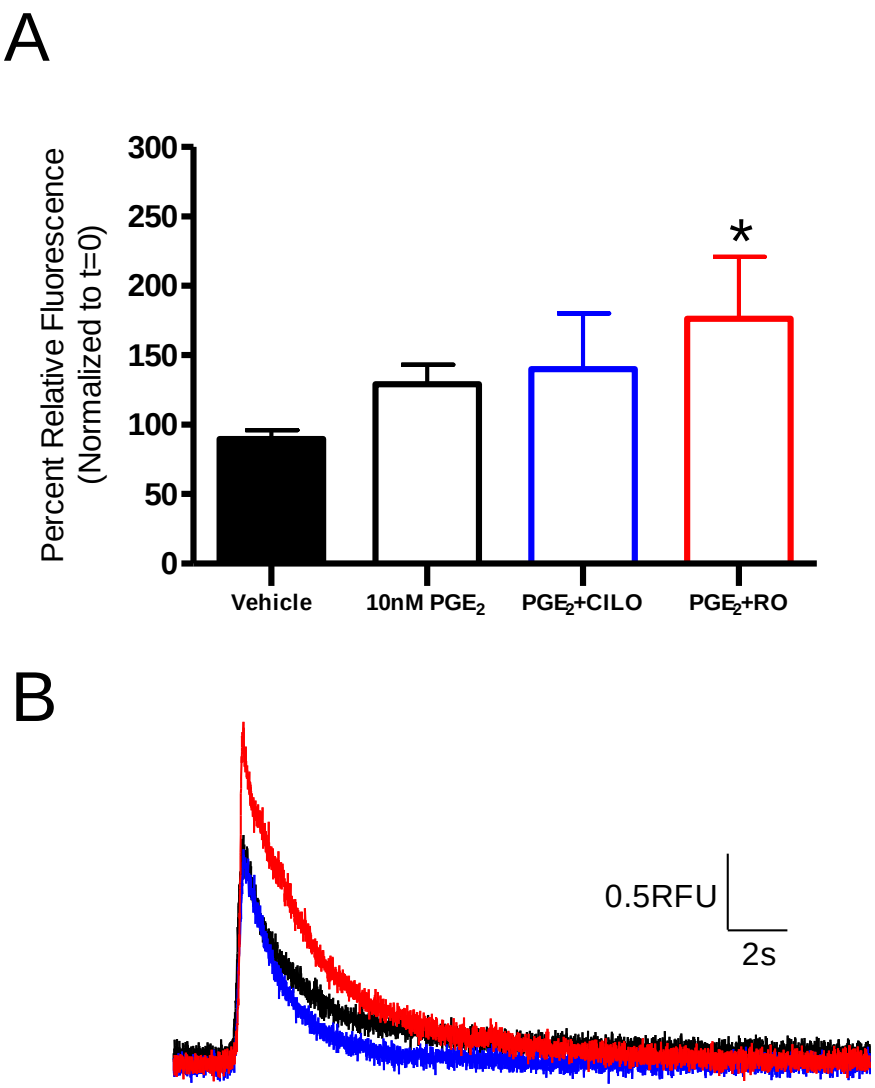

Figure 6. The Effect of PDE Inhibition on PGE_2 Enhanced SR calcium load. Right ventricular myocytes were continuously perfused with Tyrode's and field stimulated at 1 Hz. This was stopped during caffeine pulses. Panel A: The effect of vehicle, PGE_2 (10 nM), PGE_2 and cilostamide (10 nM and 1 µM, respectively), and PGE_2 and Ro 20-1724 (10 nM and 10 µM, respectively). Data are expressed as a percentage of the caffeine transient at t=0, the time at which the agonist was added to the superfusion solution. Values represent the mean ± SEM for n=5 experiments. (*) indicates data that is significantly different ($p<0.05$) from vehicle data. Panel B: Representative data of a caffeine transient at t=15 for vehicle control (black), cilostamide (blue), and Ro 20-1724 (red). Units are expressed in relative fluorescence units (RFU).

Cilostamide further increased SR load to 140 ± 41% (n=5) of t=0 values. However, neither values were significantly different from vehicle. In contrast, Ro 20-1724 led to an increase in SR load of 156 ± 47% (n=5) of t=0 values, which was a significantly greater than vehicle or 10 nM PGE_2 data.

Effects of PDE Inhibition and PGE_2 on the L-Type Calcium Current

To investigate the role of PDEs at the level of external calcium entry, we used the perforated patch-clamp technique to record L-type calcium currents (Figure 7A,B). The use of perforated patch techniques significantly attenuates the rundown of $I_{Ca,L}$ known to occur during whole cell configuration. In myocytes not pre-treated with PDE inhibitors, 10 minutes exposure of PGE_2 did not significantly alter peak inward $I_{Ca,L}$ reaching values of, at +10 mV, -6.4 ± 0.7 pA/pF (n=5), compared to -6.4 ± 0.6 pA/pF (n=5) at t=0. In the presence of Ro 20-1724, similar findings were obtained with peak currents being recorded as -6.1 ± 0.4 pA/pF (n=5) and -6.3 ± 0.6 pA/pF (n=5) for t=0 and t=10 minutes, respectively. In contrast, PGE_2 exposure to cilostamide pre-treated myocytes resulted in an insignificant increase of inward current from -6.3 ± 0.6 pA/pF (n=5) to -6.8 ± 0.5 pA/pF (n=5) over a period of 10 minutes. Sample current tracings at +10mV are shown in Figure 7C. Interestingly, myocytes pre-treated with Ro 20-1724 exhibited a slight right-ward shift of the entire current-voltage relationship that was not observed in myocytes pre-treated with cilostamide.

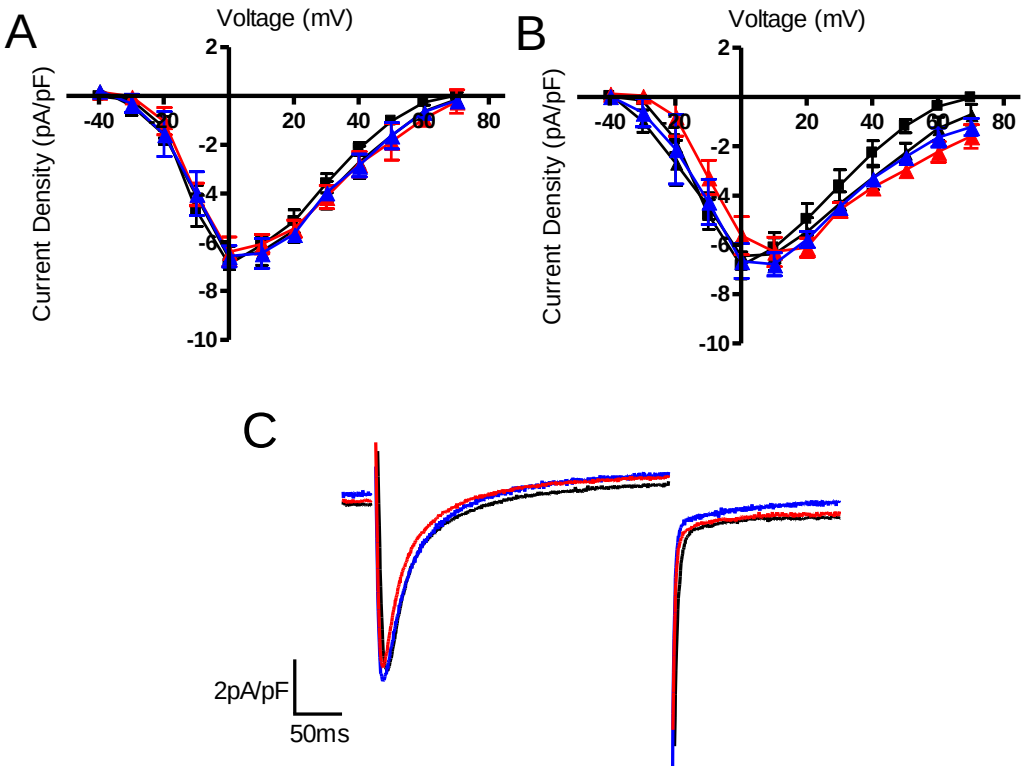

Figure 7. The Effects of PDE Inhibition on PGE_2 Enhanced L-Type Calcium Current. Cells were continuously superfused with Tyrode's solution and stimulated under voltage-clamp in a perforate patch configuration. Current-voltage relationships at t=0 (Panel A) and t=10 (Panel B) are shown with vehicle (■); PGE_2 (10 nM; ▲); PGE_2 and cilostamide (10 nM and 1μM respectively; ▲); and PGE_2 and Ro 20-1724 (10 nM and 10 μM respectively; ▲). Data has been normalized for capacitance and is expressed in pA/pF. Values represent the mean ± standard error of the mean for n=5 experiments. (*) represents data that is significantly different ($p<0.05$) from vehicle. Panel C: Representative data showing the effects of vehicle (black), PGE_2 and cilostamide (blue), and PGE_2 and Ro 20-1724 (red) on peak $I_{Ca,L}$ at +10 mV.

CHAPTER 4: FORSKOLIN RESULTS

Direct Adenylate Cyclase Agonist – Forskolin (FSK)

FSK Concentration Response Curve

Following investigations using the receptor mediated agonist PGE_2, we decided to obtain a more general understanding of PDE activity in the cell by increasing global concentrations of cAMP using forskolin (FSK), a direct adenylate cyclase agonist. As with PGE_2, we began by creating a concentration-response curve using unloaded cell shortening as an indicator of cellular contractility (Figure 8A). 30 nM FSK, 100 nM FSK, and 300 nM FSK all increased unloaded cell shortening, with values of 133 ± 10% (n=5), 175 ± 25% (n=5), and 280 ± 29% (n=5) of pre-treatment values (t=0), respectively. 1 μM FSK did not further increase cell shortening beyond 250 ± 22% (n=5) of t=0. However, there was evidence for calcium overload at 1 μM FSK, with four out of five cells demonstrating pre-contractions. A sample tracing demonstrating this effect is shown in Figure 8B. We thus concluded that a concentration of 30 nM would be appropriate for subsequent experiments using FSK and PDE inhibitors, as it elicited minimal effects on cell shortening.

Effects of PDE Inhibitors on FSK enhanced Cell Shortening

Using the same method as with PGE_2, cell shortening was measured, but with FSK as the agonist (Figure 9A). Cells were continuously superfused with Tyrode's and field stimulated at 1Hz. Use of 30 nM FSK alone increased percent shortening to 133 ± 10% (n=5) of t=0, whereas pre-treatment with cilostamide (1 μM) led to a significant

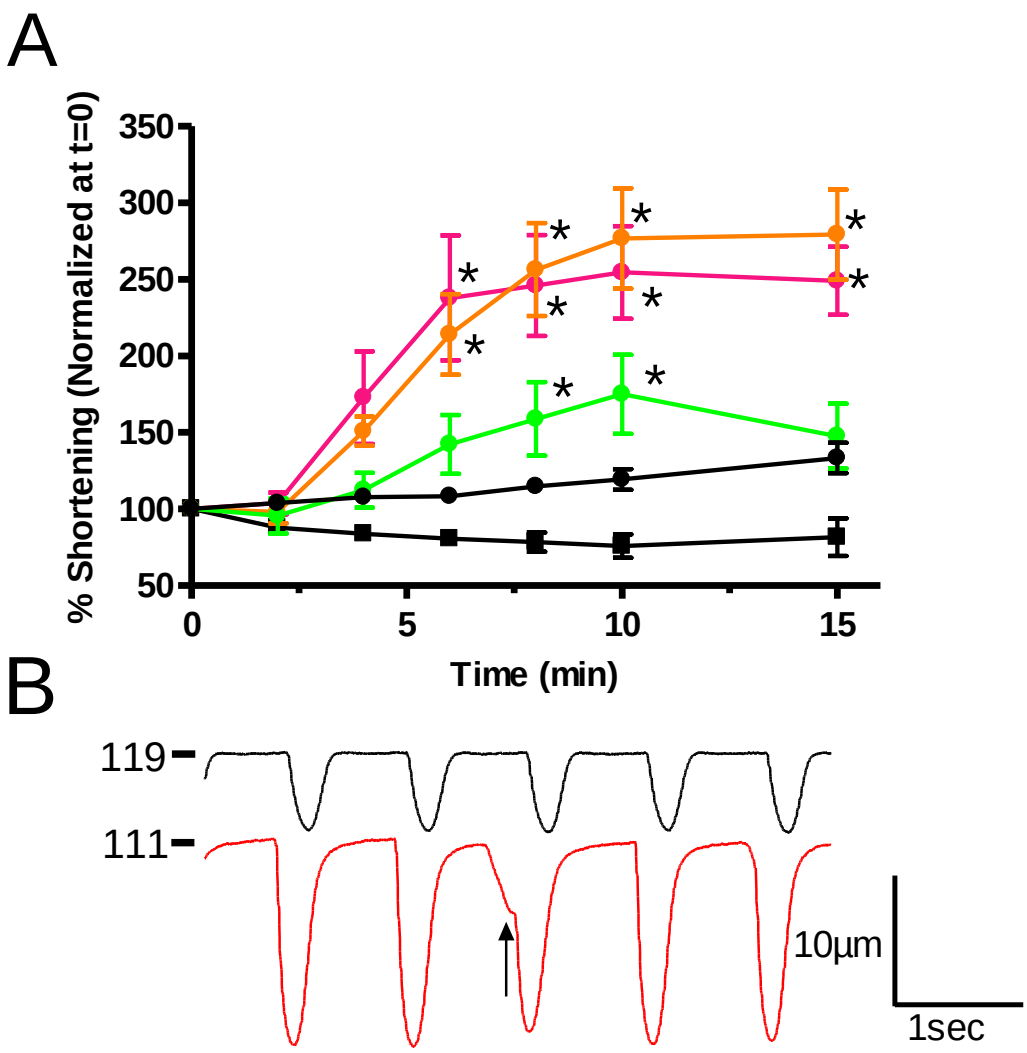

Figure 8. Concentration-Dependent Effects of Forskolin on Cell Shortening. Myocytes were superfused with Tyrode's and continuously field stimulated at 1 Hz. Various concentrations of FSK were then added to the superfusion solution for fifteen minutes (Panel A): vehicle (■); 30 nM (●); 100 nM (●); 300 nM (●); and 1 µM (●). Data are expressed as a percentage of unloaded cell shortening relative to t=0, the time at which the agonist was added to the superfusion solution. Values represent the mean ± SEM for n=5 experiments. (*) indicates data that is significantly different ($p<0.05$) from vehicle data. Panel B: Representative data illustrating the effects of 1 µM FSK on cell shortening. Sample tracings were recorded at t=0 (black) and t=15 (red). Diastolic cell lengths (µm) are listed above baseline region in sample traces. Arrow indicates a pre-contraction, an early marker of calcium overload.

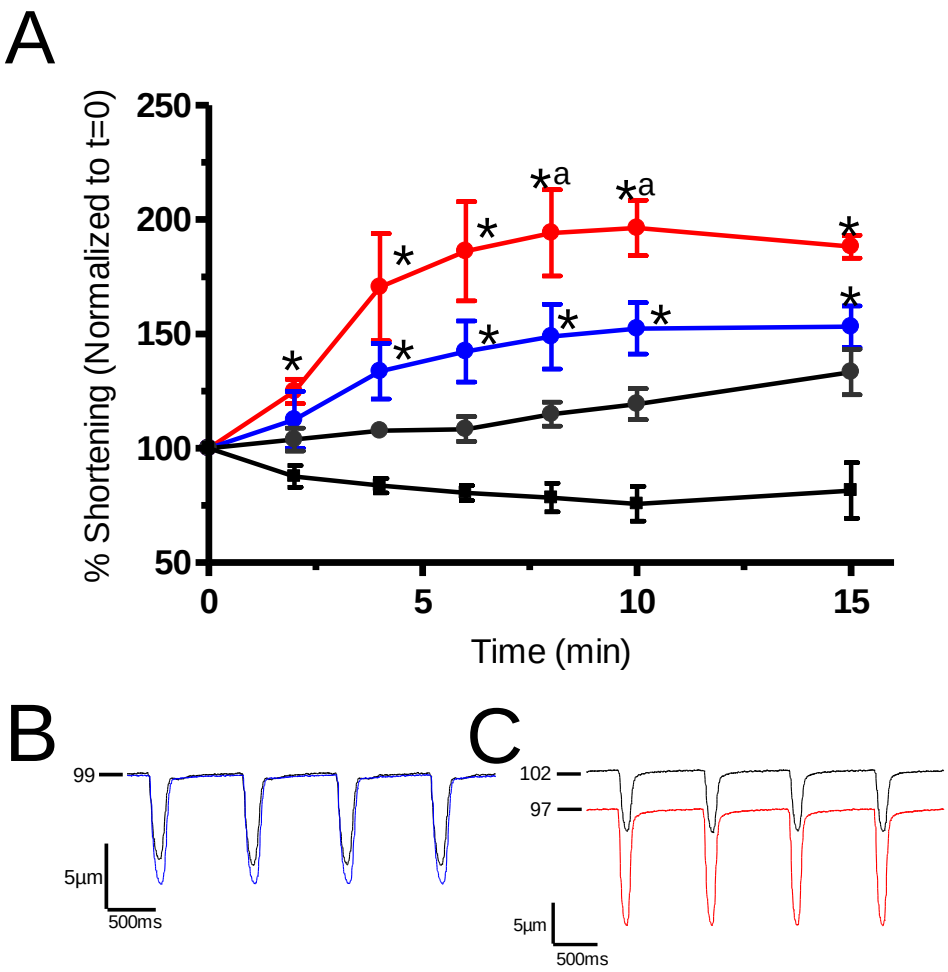

Figure 9. The Effects of PDE Inhibition on Forskolin Enhanced Cell Shortening. Ventricular myocytes were superfused with Tyrode's and continuously field stimulated at 1 Hz. Panel A: The effects of vehicle (■), FSK (30 nM; ●), FSK and cilostamide (30 nM and 1 µM, respectively; ●), and FSK and Ro 20-1724 (30 nM and 10 µM, respectively; ●) are shown. Data are expressed as a percentage of unloaded cell shortening relative to t=0, the time at which FSK was added to the superfusion solution. Values represent the mean ± SEM for n=5 experiments. (*) indicates values that are significantly different ($p<0.05$) from 30 nM FSK, and (a) indicates those values significantly different ($p<0.05$) from the combined FSK and cilostamide group. Representative data illustrating the effects of FSK and cilostamide (Panel B) and FSK and Ro 20-1724 (Panel C) are shown. Sample tracings were recorded pre-FSK at t=0 (black) and post-FSK and PDE treatment at t=15 (blue and red). Diastolic cell lengths (µm) are listed above baseline region in sample traces.

increase in cell shortening to 153 ± 9% (n=5) of t=0. Use of Ro-20-1724 (10 μM) further increased cell shortening, where a peak of 189 ± 20% (n=5) of t=0 was observed. Sample traces shown in Figure 9B,C. There was no evidence of calcium overload.

Effects of PDE Inhibitors and FSK on Calcium Transients

We then assessed the effects of PDE inhibitors and FSK on calcium transients (Figure 10). Myocytes were pre-incubated with fluo3-AM, and intracellular calcium transients recorded using a microflurometer. Superfusion with 30 nM FSK elicited an increase in peak calcium transient amplitude values to 107 ± 2% (n=5) of t=0. Pre-treatment with cilostamide did not further enhance this response, with a peak transient value of 112 ± 5% (n=5) of t=0. However, a significant increase of 145 ± 14% (n=5) of t=0 was observed using Ro-20-1724.

Effects of PDE Inhibitors and FSK on SR Loading

We then evaluated the effects of PDE inhibitors and FSK on SR calcium loading. Cells were incubated with fluo3-AM, and then superfused with Tyrode's solution. A 100 mM caffeine pulse was used to initiate SR calcium unloading, and the corresponding increase in fluorescence was measured. This was done twice, once at t=0 (pre-FSK application) and t=10 (post-FSK application), and final values were expressed as a percent change from t=0 to t=10 as shown in Figure 11.

Superfusion with 30 nM FSK increased SR load to 103 ± 14% (n=5) of t=0 from a value of 89 ± 14% (n=5) of t=0 for vehicle control cells. Cilostamide was not

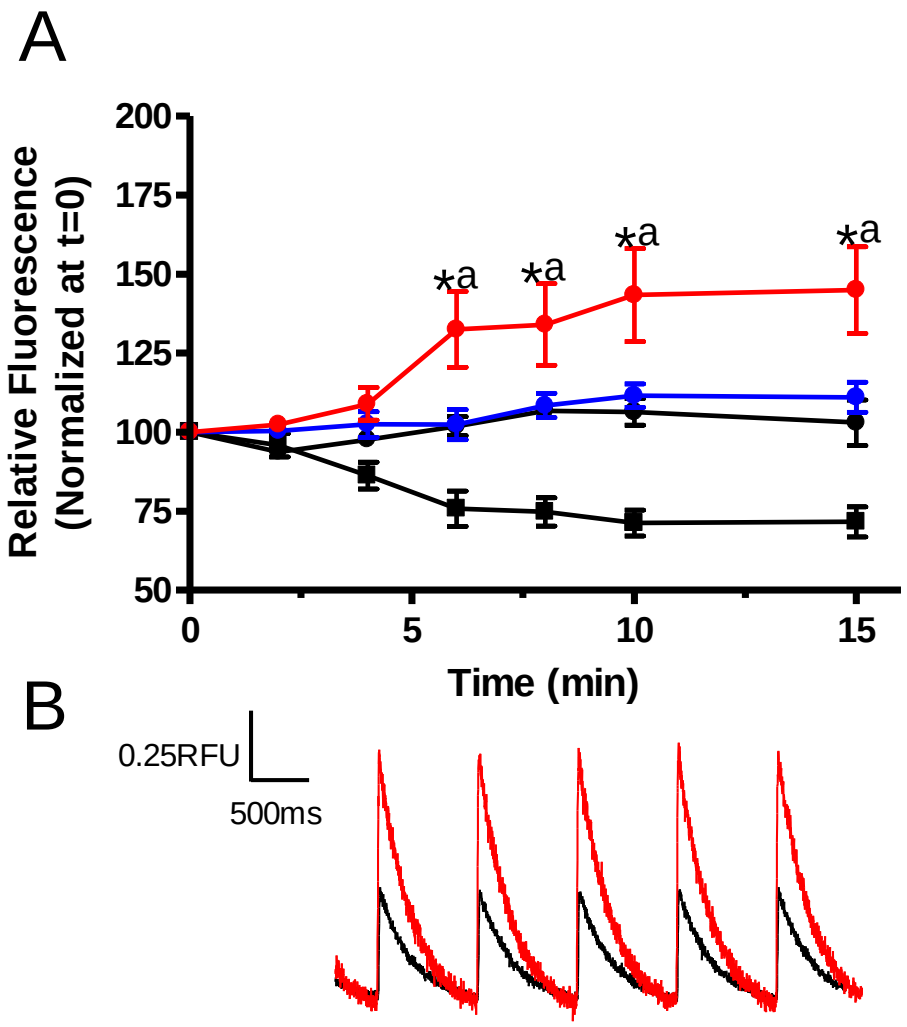

Figure 10. The Effects of PDE Inhibition and Forskolin on Intracellular Calcium Transients. Ventricular myocytes were superfused with Tyrode's solution and continuously field stimulated at 1 Hz. Panel A: Effects of vehicle (■), FSK (10 nM; ●), FSK and cilostamide (30 nM and 1 µM, respectively; ●), and FSK and Ro 20-1724 (30 nM and 10 µM, respectively; ●). Data are expressed as a percentage of peak calcium transient relative to t=0, the time at which the agonist was added to the superfusion solution. Values represent the mean ± SEM for n=5 experiments. (*) indicates data that are significantly different ($p<0.05$) from 30 nM FSK data, and (a) reflect those values significantly different ($p<0.05$) from the combined FSK and cilostamide group. Panel B: Representative data illustrating the effects of Ro 20-1724 pre-FSK (black) and post-FSK (red) at t=15. Units are expressed in relative fluorescence units (RFU).

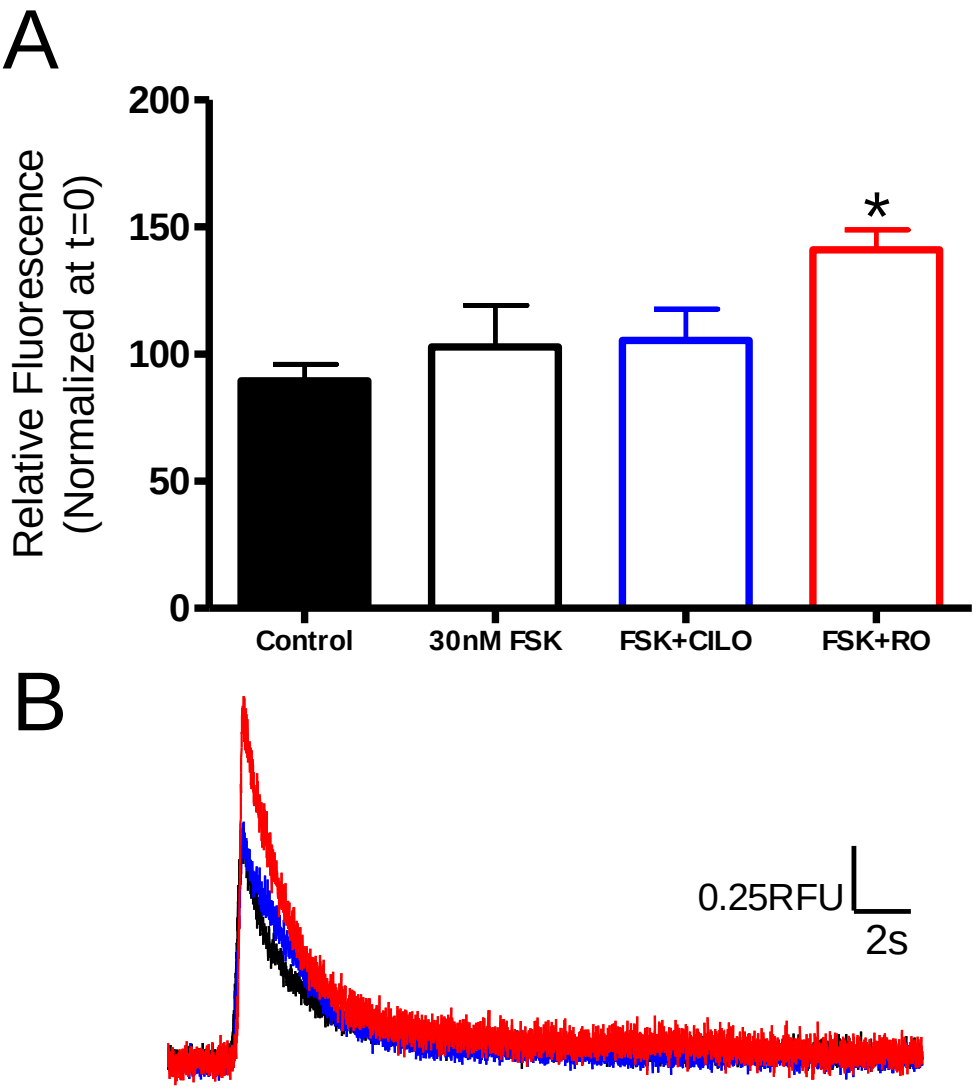

Figure 11. The Effect of PDE Inhibition on FSK Enhanced SR Calcium Load. Right ventricular myocytes were continuously perfused with Tyrodes and field stimulated at 1 Hz. This was stopped during caffeine pulses. Panel A: The effect of vehicle control, FSK (30 nM), FSK and cilostamide (30 nM and 1 µM, respectively), and FSK and Ro 20-1724 (30 nM and 10 µM, respectively). Data are expressed as a percentage of the caffeine transient at t=0, the time at which the agonist was added to the superfusion solution. Values represent the mean ± SEM for n=5 experiments. (*) indicates data that is significantly different ($p<0.05$) from control data. Panel B: Representative data of a caffeine transient at t=15 for control (black), cilostamide (blue), and Ro 20-1724 (red). Units are expressed in relative fluorescence units (RFU).

significantly different, with an increase of 105 ± 12% (n=5) of t=0. However, PDE4 inhibition with Ro 20-1724 increased SR loading significantly to 127 ± 11% (n=5) of t=0. This pattern is similar to what was observed using PGE_2 as an agonist.

Effects of PDE Inhibitors and FSK on L-Type Calcium Currents

L-type calcium ($I_{Ca,L}$) currents were recorded using a perforated patch clamp configuration (Figure 12A,B). Superfusion with 30 nM FSK did not significantly alter peak inward $I_{Ca,L}$ reaching values of, at +10 mV, -6.6 ± 0.3 pA/pF (n=5), compared to -6.3 ± 0.5 pA/pF (n=5) at t=0. In the presence of cilostamide, similar findings were obtained with peak inward currents being recorded as -6.2 ± 0.3 pA/pF (n=5) and -6.4 ± 0.2 pA/pF (n=5) for t=0 and t=10 minutes, respectively. In contrast, FSK exposure to Ro 20-1724 pre-treated myocytes resulted in a significant increase of inward current from -6.0 ± 0.8 pA/pF (n=5) to -7.7 ± 0.4 pA/pF (n=5) over a period of 10 minutes. Representative traces of peak $I_{Ca,L}$ are shown in Figure 12C.

Furthermore, myocytes pre-treated with either Ro 20-1724 or cilostamide exhibited a slight right-ward shift of the current-voltage relationship that was not observed in either the control or 30 nM FSK groups.

Effects of PDE Inhibition and FSK on Potassium Currents

We also investigated potassium currents and action potentials. This was done to ensure that the changes in cell shortening were not due to changes in potassium conductance. Thus, we chose FSK as our agonist because it would definitively increase

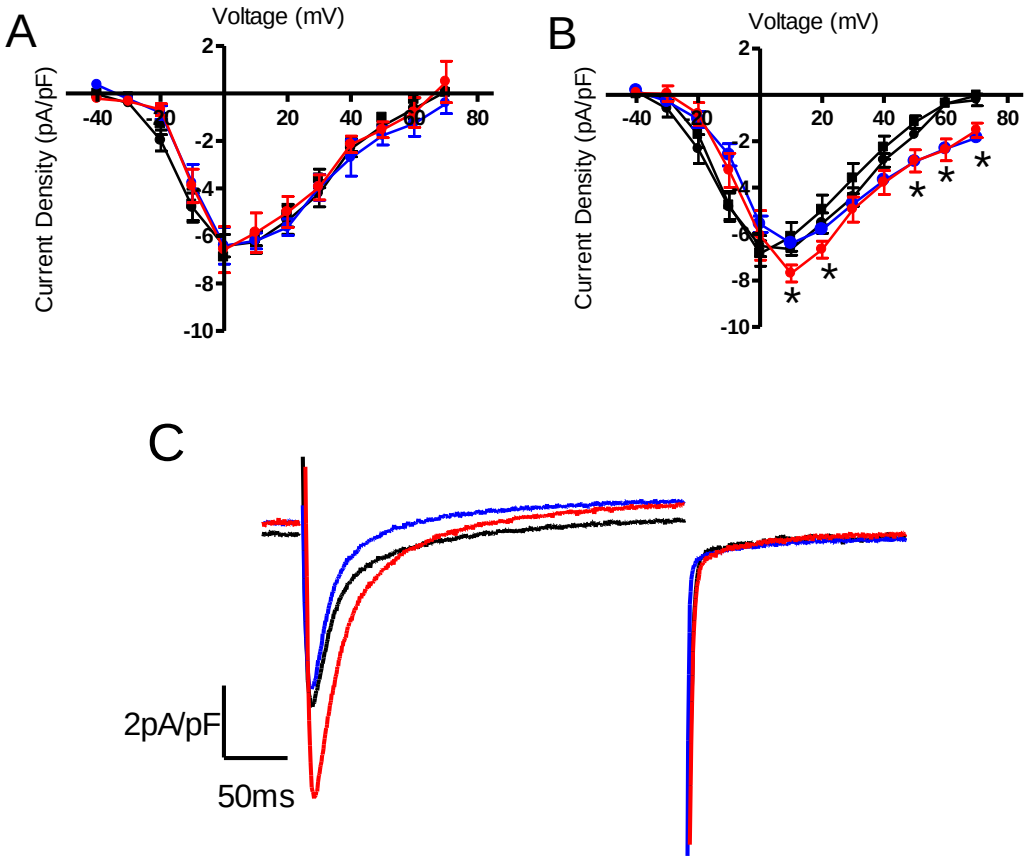

Figure 12. The Effects of PDE Inhibition on Forskolin Enhanced L-Type Calcium Current. Cells were continuously superfused with Tyrode's solution and stimulated under voltage-clamp in a perforated patch configuration. Current-voltage relationships at t=0 (Panel A) and t=10 (Panel B) are shown with vehicle (■); FSK (30 nM; ●); FSK and cilostamide (30 nM and 1 µM respectively; ●); and FSK and Ro 20-1724 (30 nM and 10 µM respectively; ●). Data has been normalized for myocyte capacitance and is expressed in pA/pF. Values represent the mean ± standard error of the mean for n=5 experiments. (*) represents data that is significantly different ($p<0.05$) from 30 nM FSK. Panel C: Representative data showing the effects of vehicle control (black), FSK and cilostamide (blue), and FSK and Ro 20-1724 (red) on peak $I_{Ca,L}$ at +10 mV.

cAMP concentrations, and would provide the most robust response if changes in potassium conductance were present.

We measured three major potassium currents found in the rat ventricular myocyte: the transient outward (I_{to}), inward rectifier (I_{K1}), and delayed rectifier (I_{sus}). Though potassium currents do not generally display rundown, we used perforated patch both for consistency and to prevent dialysis of the second messenger molecules involved in the cAMP signalling pathway.

Cells were treated with FSK and PDE inhibitors using the same time intervals as previously stated. Current-voltage (IV) relationships were recorded pre-FSK at t=0, and post, at t=10. As expected, there was no change in the IV relationship of all three currents (Figure 13) with and without PDE inhibitors (all trials n=3).

In control cells, measured I_{to} values, at +50mV, were 16.7 ± 1.5 pA/pF at t=0. This was unchanged at t=10, with outward currents of 17.7 ± 0.7 pA/pF. When pre-treated with 30 nM FSK, I_{to} values were 17.6 ± 1.3 pA/pF at t=0, and remain unchanged at t=10, 16.4 ± 3.1 pA/pF. Similarly, pre-treatment with cilostamide elicited currents of 15.7 ± 0.7 pA/pF at t=0, with no significant change at t=10, 15.9 ± 1.5 pA/pF. Those treated with Ro 20-1724 also exhibited no change, with currents of 15.2 ± 1.0 pA/pF at t=0 and 15.0 ± 0.7 pA/pF at t=10.

I_{K1} also was not significantly different from vehicle control when treated with 30 nM FSK. Inward current, at -120 mV, was -9.3 ± 1.4 pA/pF at t=0 and -10.7 ± 1.6 pA/pF at t=10. When cells were pre-treated with cilostamide, we observed currents of -9.3 ± 0.2 pA/pF at t=0. This was unchanged at t=10, -9.4 ± 1.8 pA/pF. Similarly, pre-

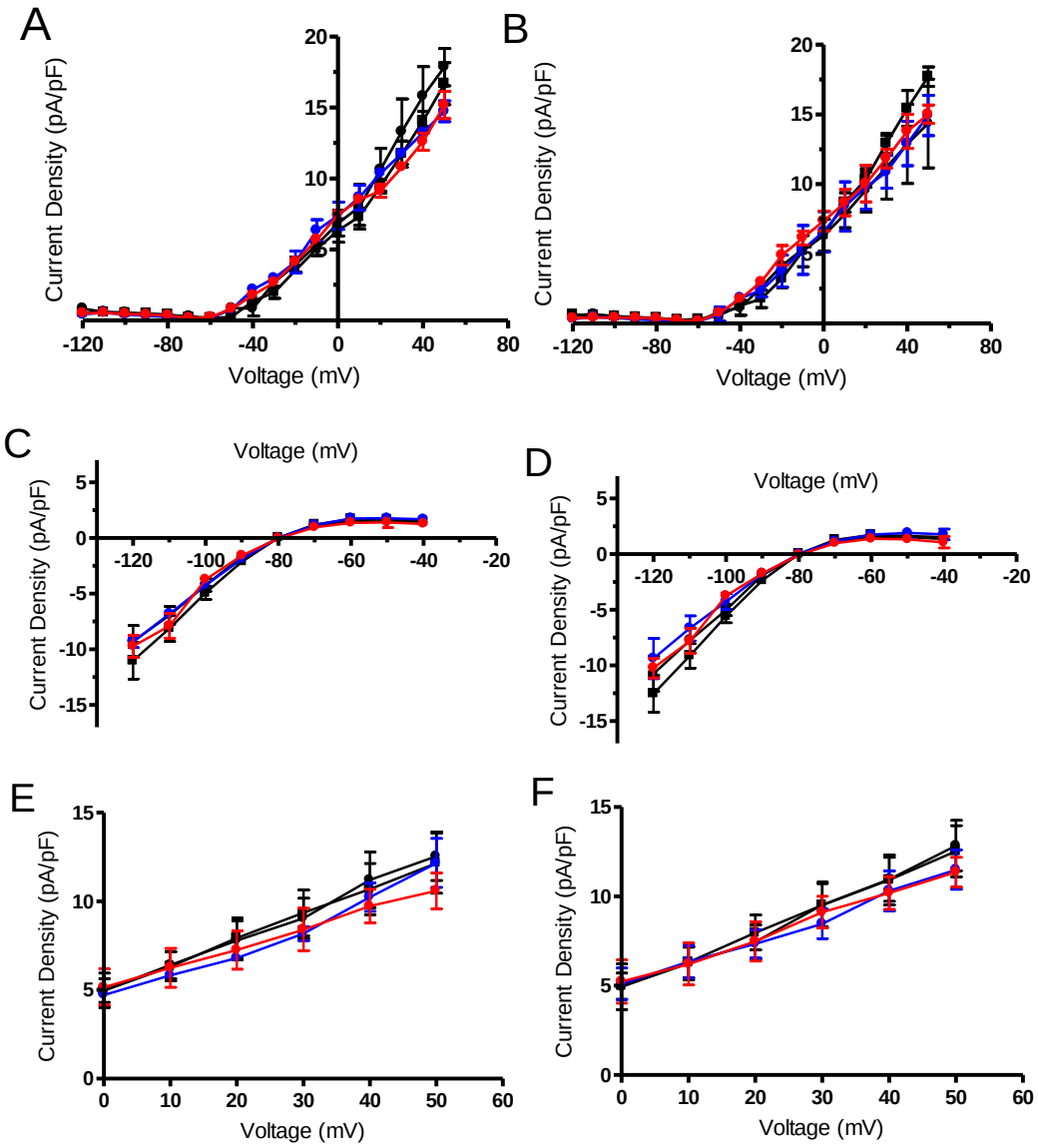

Figure 13. The Effects of PDE Inhibition on Forskolin Enhanced Potassium Currents. Right ventricular myocytes were continuously superfused with Tyrode's solution and stimulated under voltage-clamp using the perforated patch configuration. Cells were treated with vehicle (■); FSK (30 nm; ●); FSK and cilostamide (30 nm and 1 µM, respectively; ●); or FSK and Ro 20-1724 (30 nM and 10 µM, respectively; ●). Current-voltage relationships for I_{to}, I_{K1}, and I_{sus} at t=0 are shown in Panels A, C, and E, respectively. Current voltage relationships at t=15 for I_{to}, I_{K1}, and I_{sus} are shown in Panels B, D, and F, respectively. Data has been normalized for capacitance, and is expressed in pA/pF. Values represent the mean ± standard error for n=3.

treatment with Ro 20-1724 yielded -9.7 ± 0.1 pA/pF at t=0, and -10.2 ± 0.8 pA/pF at t=10.

Lastly, I_{sus} outward current, at +50 mV, did not change from t=0 values, 12.5 ± 1.4 pA/pF, following 10 minutes perfusion with 30 nM FSK, 12.8 ± 1.4 pA/pF. Pre-treatment with cilostamide also did not alter I_{sus}, with inward currents of 12.2 ± 1.4 pA/pF at t=0, and 11.5 ± 1.1pA/pF at t=10. Cells pre-treated with Ro 20-1724 remained unchanged as well, with observed currents of 10.6 ± 1.0 pA/pF at t=0, and 11.4 ± 0.8 pA/pF at t=10.

Effects of PDE Inhibition and FSK on Action Potentials

Under the same recording conditions of potassium currents, action potentials were elicited using a depolarizing 700pA current injection during current-clamp. The APD90, defined as the time it takes for the cell to repolarize to 90%, from peak to the resting membrane potential, was calculated for each cell. These values were then expressed as a percent change from t=0 to t=10, (Figure 14). The average change in APD90 was 98 ± 7% (n=3) of t=0 for FSK alone, 100 ± 2% (n=3) of t=0 for cells pre-treated with cilostamide, and 104 ± 3% (n=3) of t=0 for those with Ro 20-1724. None of these were significantly different from vehicle.

Effects of IBMX and Combined PDE3 and PDE4 Inhibition on Cell Shortening

In addition to selective inhibition, we also wanted to evaluate the effects of inhibiting multiple PDEs simultaneously (Figure 15). This was with the intention of

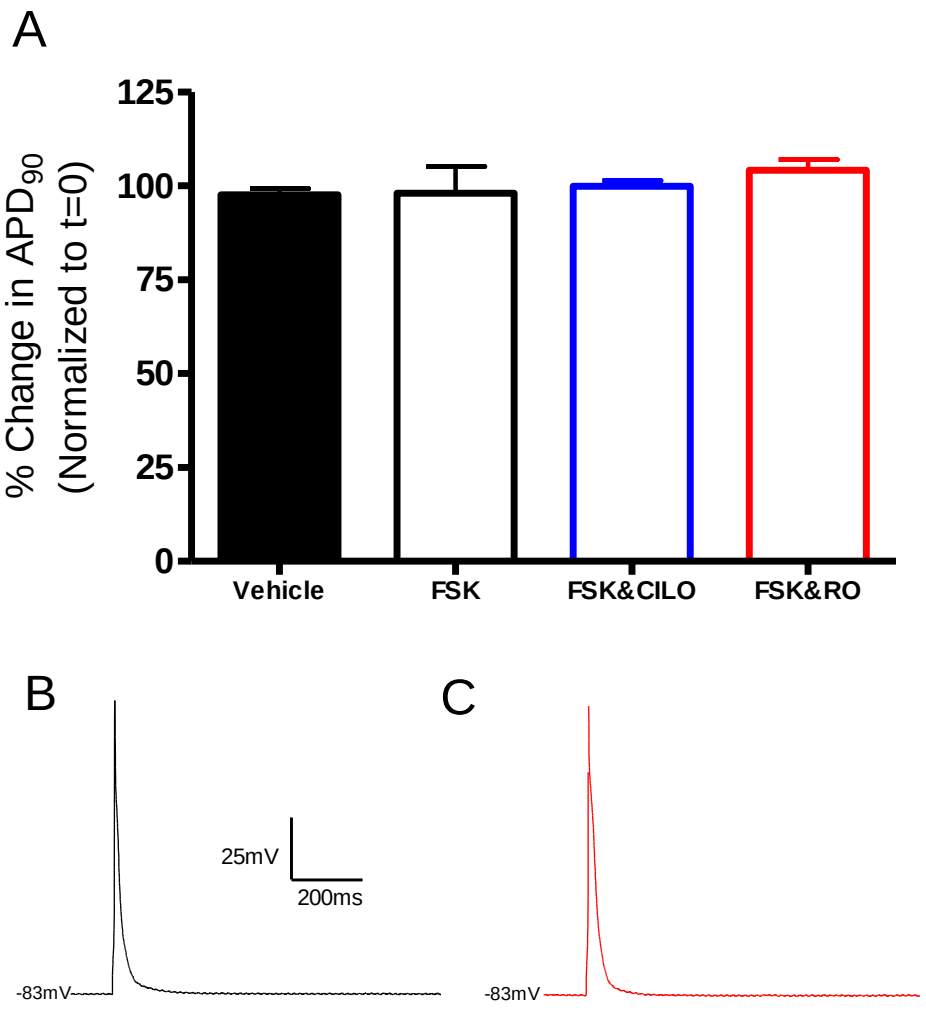

Figure 14. The Effects of PDE Inhibition on Forskolin Enhanced APD90. Right ventricular myocytes were continuously superfused with Tyrode's solution and field stimulated at 1 Hz. Panel A: The percent change in APD90 when treated with vehicle, FSK (30 nM); FSK and cilostamide (30 nM and 1 µM, respectively); and FSK and Ro 20-1724 (30 nM and 1 µM, respectively). Data is expressed as a percent of value at t=0. Values represent the mean ± SEM for n=5 experiments. Also shown, representative data of action potential for vehicle cell (Panel B, black) and cell pre-treated with Ro 20-1724 (Panel C, red), both at t=10.

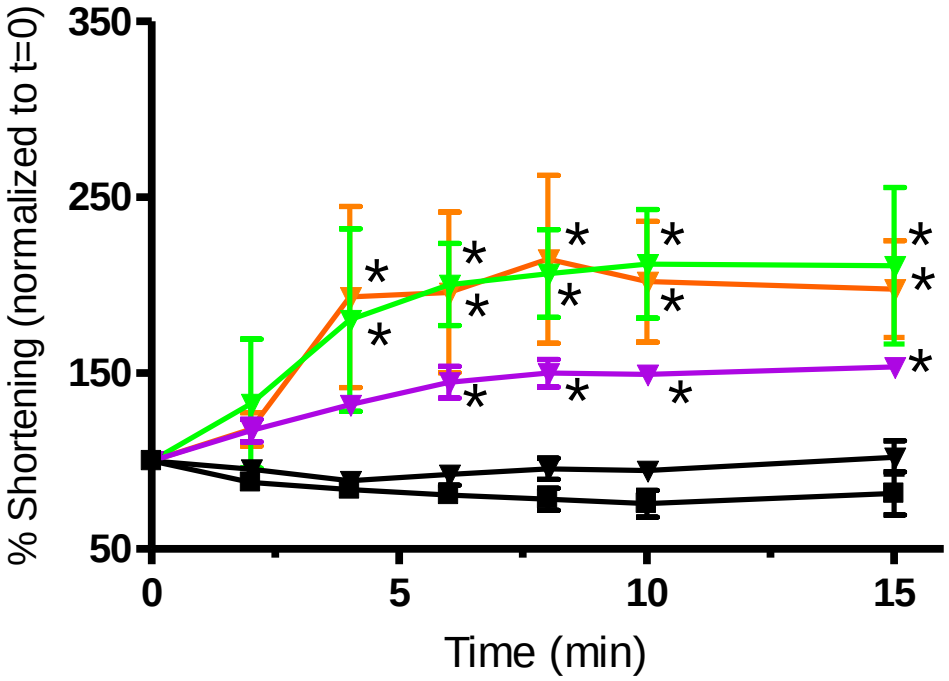

Figure 15. Effects of Multiple PDE Inhibition on Cell Shortening. Right ventricular myocytes were continuously superfused with Tyrodes solution and field stimulated at 1 Hz. Various concentrations of IBMX were added to the superfusion solution: vehicle (■); 1 µM (▼); 50 µM (▼); and 100 µM (▼). 10 µM Ro 20-1724 combined with 1 µM cilostamide (▼) are also shown. Data are expressed as a percentage of unloaded cell shortening relative to t=0, the time at which the PDE inhibitor was added to the superfusion solution. Values represent the mean ± SEM for n=5 experiments. (*) indicates values that are significantly different ($p<0.05$) from vehicle data.

determining if different PDEs were involved in the regulation of the responses observed in the previous experiments. We began by assessing the concentration-dependent effects of isobutylmethylxanthine (IBMX), a global PDE inhibitor, on cell shortening. 10 minutes superfusion with 1 μM IBMX failed to elicit any significant differences from vehicle control, with cell shortening values of 94 ± 6% of pre-treatment (t=0) values. However, 50 μM IBMX significantly increased this value to 212 ± 31% of t=0. Further increases with 100 μM IBMX was not observed, with cell shortening values of 202 ± 34%. Additionally, 3 of 5 cells reached calcium overload with 50 μM IBMX, and 4 out of 5 with 100 μM. This indicates that cellular regulation was dysfunctional, and therefore would be unsuitable for agonist enhanced experiments.

Thus, we attempted using a combination of cilostamide (1 μM) and Ro 20-1724 (10 μM), since PDE3 and PDE4 are responsible for the majority of PDE activity (Mongillo et al, 2004). However, 10 minutes superfusion of this treatment significantly increased cell shortening values to 154 ± 4% of t=0. Thus, since both approaches appear to significantly increase cell shortening, we were unable to assess the effects of multiple PDE inhibitors on agonist enhanced cellular parameters using a pharmacological method.

CHAPTER 5: DISCUSSION AND FINAL REMARKS

Summary

The heterogeneity of responses provided by the myriad of unique receptor agonists despite exploiting the same second messenger, cAMP, has been primarily attributed to compartmentation of the signal within a cell. Though much remains debated, it is generally agreed that PDEs function to delineate cAMP diffusion to certain targets to prevent the unspecified effects. However, what has been lacking in the literature is an understanding of where PDEs are localized within various subcellular compartments, and whether their activity varies depending on the agonist. We sought to investigate these receptor specific effects by using prostaglandin E_2 (PGE_2) as an alternative GPCR mediated agonist to contrast with previous work done using the β-AR stimulus, isoproterenol (ISO). Our results have demonstrated that the cellular responses to PDE inhibition do in fact depend on the pathway being activated.

Specifically, our results indicate that a unique signal relies not only on the localization of PDE isoforms to subcellular compartments, but on the location of the receptor itself. Our findings thus support a 'barrier' compartmentation hypothesis, where PDEs function as a wall to cAMP concentration which decreases from its site of production. For instance, β-AR are most likely localized to the t-tubules, whereby adenylate cyclates can exert effects on mechanisms involved primarily in excitation-contraction coupling. On the other hand, the prostanoid receptors, EP_2 and EP_4, are located further away from t-tubules and the sarcomere, but may be closer to the nucleus where PGE_2 exerts its effects. This is illustrated in the diagram (Figure 16) below.

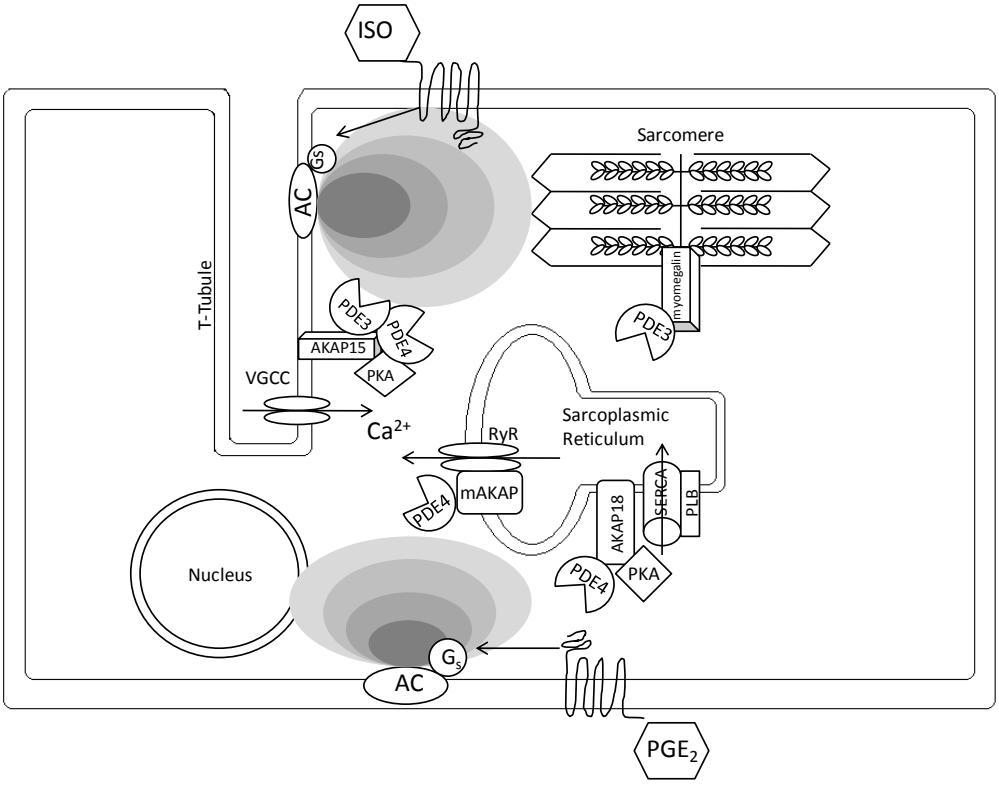

Figure 16. Conceptual model for the localization of PDEs and receptors in β-adrenergic and EP receptor pathways in cardiac ventricular myocytes. Our study suggests that pathway specificity is a function of strategically placed receptors, adenylate cyclases, and PDEs near their typical targets to create the unique effects associated with each distinct receptor agonist. We propose that β-adrenergic receptors are located at the t-tubules to exert effects on ECC mechanisms, whereas EP receptors are situated closer to the nucleus. PDE4 is uniquely associated with the SR PDE3 at the sarcomere, and a combination of the two at the LTCC. Proposed scaffolding mechanisms are speculations based on current literature review.

Compartmentation with Receptor Mediated Agonists: Effects of PDE Inhibitors on PGE_2 Enhanced Cellular Parameters

We investigated how various cellular parameters would respond to PDE inhibition when treated with a receptor mediated agonist. Previous work using the archetypal β-adrenergic agonist, isoproterenol (ISO), has shown that a distinct pattern of PDE activity was responsible for the compartmentation of the cAMP signal (Schwartz J. Unpublished Data, 2007). As an extension of this work, we chose to investigate whether a different pattern would emerge using an alternative GPCR agonist, prostaglandin E_2 (PGE_2), which targets the EP_2 and EP_4 receptors on the myocyte membrane (Bos et al, 2004). This compound was chosen because although it exploits the cAMP/PKA signalling cascade, its downstream effects are very different than the positive inotropy associated with the β-adrenergic response. In fact, PGE_2 is better known for its action in the nucleus, where it initiates responses related to inflammation, such as ventricular remodelling and hypertrophy (Mendez et al, 2002). This is accomplished without significantly altering myocyte contractility (Klein et al, 2004), thus making it an interesting contrast to ISO.

Before experimenting with PDE inhibitors, a concentration-dependent response in cell shortening was observed. As expected, PGE_2 failed to elicit large changes in percent shortening where 1μM PGE_2 resulted in cell shortening values of 125%. This contrasts with what has been shown using ISO, where a concentration of 30 nM resulted in a peak percent shortening of 320%. These findings are relevant because based on our experience cell shortening rarely exceeds 350%. This is likely due to a physical

limitation in sarcomere interaction, and when this does occur, myocytes exhibit what we term calcium overload. Such characteristics of overload include spontaneous contractions, shorter resting length, and unusual electrical activity, all of which are indications of disorganized calcium signalling. PGE_2 did not result in any overload at any concentrations, whereas ISO begins to exhibit it at concentrations higher than 30 nM. This difference indicates that a discrete pattern of regulation exists for both pathways.

Thus, these results confirm that PGE_2 is not a potent positive inotropic agent, and could be due to several reasons. For instance, weak coupling between G_s and ACs could result in reduced cAMP production. However, some studies have suggested that cAMP production is too diffuse to account for the distinct subcellular pools (Zaccolo et al, 2002). Thus, we postulated that the receptor is specifically localized to distinct subcellular domains, and that specific PDEs help limit the diffusion of cAMP near those cellular parameters that are not generally targets of that agonist.

Deciding to investigate the former, we began by assessing the effects of PDE inhibitors on PGE_2 enhanced cell shortening. Interestingly, there was an increase in unloaded cell shortening with Ro 20-1724, a selective PDE4 inhibitor, but none was observed using cilostamide, a selective PDE3 inhibitor. Thus, we hypothesized that PDE4 is the main PDE that delineates cAMP diffusion to ECC mechanisms when there is an activation of the EP receptor. We decided to investigate exactly which mechanisms were being targeted through fluorescent calcium imaging.

We demonstrated that PGE_2 enhanced calcium transients increased under PDE4 inhibition, confirming that certain targets are indeed acting to increase intracellular

calcium. Interestingly, our results indicate that this is almost entirely attributed to PDE4 association with the SR, since no change was found in the L-Type calcium current ($I_{Ca,L}$). The specifics of PDE4 association with the SR will be discussed in detail later. Nonetheless, we can conclude that the PGE_2 pathway most likely achieves the small increase in contractility by increasing SR loading, not through changes in calcium current.

Our findings regarding $I_{Ca,L}$ lead to conclusions that contradict our original hypothesis that cAMP production is too diffuse to account for compartmentation. Work done by Rochais et al (2006) also showed that neither PDE3 nor PDE4 affected PGE_1 stimulation, another EP receptor agonist. Thus, we postulate that EP receptors lie in a distinct subcellular compartment from calcium channels, and that the physical distance prevents an effective cAMP concentration from reaching the LTCC.

Global PDE Activity: The Effects of PDE Inhibitors on FSK Enhanced Cellular Parameters

Biochemical studies have shown that by activity both PDE3 and PDE4 provide most of the activity in rat cardiac ventricular myocytes, approximately 80-90% (Mongillo et al, 2004). However, we wanted to assess whether a different pattern would emerge when various compartmentalized functions were isolated. Thus, we chose to repeat the same experiments as we did with PGE_2, but with forskolin (FSK), a direct AC agonist. This would bypass any receptor specific activity, and provide us with a more general idea of PDE activity in the cell.

Overall, we have shown that both PDE3 and PDE4 are indeed present in the cell. However, PDE4 appears to be responsible for the majority of cAMP hydrolysis. Further, we confirmed our previous conclusion that it plays a singular role at the SR. Also, we have shown that PDE4 is more important than PDE3 at the level of the LTCC, which is consistent with earlier studies showing that rat ventricular tissue does not respond as robustly to PDE3 inhibition as PDE4 (Xiong et al, 2001). In human (Sugioka et al, 1994) and dog (Weishaar et al, 1987) PDE3 is the dominant isoform. However, PDE4 is dominant in the rat (Shahid & Nicholson, 1990) and frog (Lugnier et al, 1992). Thus, our findings are consistent with differences in PDE activity between species.

In addition, our results indicate that PDE3 likely functions by delineating cAMP pools at the sarcomere and contractile machinery. This is similar to what we observed using ISO as an agonist. Exactly how the PDE3 is anchored at the contractile apparatus is not well understood. However, recent work suggests that PDE4D may associated at the Z-line of the sarcomere by means of a myomegalin anchoring protein in humans (Verdi et al, 2001), and perhaps a similar mechanism is functioning in the rat.

We also demonstrated separate effects of cilostamide and Ro 20-1724 on LTCC. Both inhibitors resulted in a rightward shift of the current voltage relationship, however, only Ro 20-1724 caused an increase in the peak inward calcium current. This suggests that both PDE3 and PDE4 are localized at the t-tubules, but that PDE4 appears to be more important in the regulation of cAMP diffusion near the LTCC. This was also shown in our previous work using ISO, where inhibition of either PDEs increased $I_{Ca,L}$, however was greater with PDE4 inhibition.

Why PDE4 is the dominant isoform may be due to several reasons. For instance, it could be present in greater proportion than PDE3 at the LTCC, and thus its inhibition would have a more profound impact on cAMP diffusion. Furthermore, PDE4 is known to possess a higher K_m value than PDE3 (Reviewed in Osadchii, 2008). Consequently, as cAMP concentration increases, as it would with stimulation from ISO or FSK, PDE4 becomes more responsible for the majority of the hydrolysis. There are several studies suggesting how PDEs may be localized at the LTCC. Specifically, it has been shown that the PDE4D is localized to the rat ventricular calcium channel, $Ca_v1.2$, via the A-kinase anchoring protein, specifically AKAP15 (Hulme et al, 2003).

Given the fact that both PDE3 and PDE4 are involved in calcium current regulation, we wanted to explore the effects of combined PDE inhibitors, since it would provide an indication if one was contributing more than the other. We found that using any concentration of isobutylmethylxanthine (IBMX) above 50µM led to significant increases in cell shortening and indications of calcium overload, such as spontaneous, non-triggered contractions. This was also present when we opted to use a combination of cilostamide and Ro 20-1724. This finding is consistent with other data in the literature. It has been shown that in response to PDE3 and PDE4 inhibition together $I_{Ca,L}$ will increase significantly, but no effect is observed when either is inhibited alone (Verde et al, 1999). However, due to these results, we have concluded that global PDE inhibition can cause substantial disruptions to calcium signalling and therefore could not be further studied in combination with an additional agonist.

Interestingly, our combined PDE inhibitor studies demonstrate that PDE3 and PDE4 are the main isoforms functioning at rest in the myocyte. However, the fact that IBMX resulted in further increases in cell shortening may indicate that other PDEs, specifically PDE1 and PDE2, could be involved in regulating cAMP levels.

Finally, it had been previously shown that potassium currents function in the β-adrenergic response (Marx et al, 2002), and that the mouse I_{Ks} channel is co-localized with PDE4 and AKAP-9 (Terrenoire et al, 2009). Thus, we investigated whether there was an effect on the major potassium currents found in the ventricular myocyte, I_{to}, I_{K1}, and I_{sus}. We found no change in response to FSK, or combined with PDE inhibitors. This was also the case when using ISO as an agonist in previous work. However, the discrepancy with the literature may be due to several reasons. Particularly, I_{Ks} in the mouse is not analogous to I_{sus} in the rat, which is probably more similar to I_{Kr} (Reviewed in Barry & Nerbonne, 1996). Further, the pattern of PDE regulation could be due to differences between species (Okruhlicova et al, 1997). For instance, a different PDE isoform other than PDE3 or PDE4 could be responsible for potassium current regulation, as mentioned in discussion on our IBMX findings above.

PDE4 Activity: Special Considerations

As discussed earlier, our results suggest that PDE4 is the only PDE associated with the SR, independent of the agonist used to stimulate cAMP production. This finding deserves particular attention because it directly conflicts with the majority of current literature, which suggests that PDE3 is the main isoform localized to the SR (Lugnier et

al, 1993), and has been repeatedly shown in most mammalian species, such as dog (Kaufmann et al, 1986), rabbit (Kithas et al, 1988), and human (Movsesian et al, 1991) myocytes.

We postulate several reasons for this discrepancy. Firstly, differences in PDE activity between species are well documented (Okruhlicova et al, 1997), and currently there are no studies that have specifically assessed the role of PDEs at the SR in the adult rat ventricular myocyte. Furthermore, some groups have used whole tissue samples (Shakur et al, 2002), which can confound the specificity of PDE localization in contractile tissue. Finally, those using rat models have used cultured or neo-natal ventricular myocytes (Mongillo et al, 2004). Cultured cardiac tissue has been shown to adapt to the cell culture environment, which can change its electrical, morphological and contractile function (Banyasz et al, 2007); and, developmental changes in PDE activity are also well documented (Akita et al, 1994).

Another interesting finding was that PGE_2 was able to facilitate larger increases in SR loading than either FSK or ISO. This leads us to believe that the EP receptors are localized near the SR, and that any of the observed effects on intracellular calcium are due to alterations in SR loading. This is probably facilitated through several anchoring proteins at the SR membrane. One study has suggested that PDE4 may be localized at the SR. Kerfant and colleagues (2007) used co-immunoprecipitation experiments to show that PDE4D3 is localized at the SR through the large scaffolding protein, mAKAP, which also brings it into proximity to PKA and the ryanodine receptor (RyR). Conversely, work done in renal principal cells has shown that PDE4 can be also be

localized to SERCA via AKAP18 (Stefan et al, 2007), thereby increasing total phosphorylated phospholamban (PLB) and mediating an increase in calcium reuptake.

We propose that both mechanisms are present in the rat ventricular myocyte. Using the shape of the calcium transient, we can determine whether a change in calcium release (slope of the upstroke) or calcium reuptake (slope of the downstroke) has occurred. When compared with controls, we found that FSK exhibited changes in both release and reuptake in the presence of Ro 20-1724. However, PGE_2 only altered the downstroke. Our previous research with ISO demonstrated a change in both release and reuptake as well. This leads us to believe that both mechanisms are involved in β-adrenergic signalling, which is consistent with other studies showing that the RyR is closely associated with t-tubules and the β-adrenergic receptors (Reviewed in Orchard and Brette, 2008). However, our PGE_2 results suggest that the EP receptor is localized closer to SERCA, since PGE_2 combined with Ro 20-1724 only affected reuptake.

Finally, as mentioned previously, PDE3 possesses a lower K_m value for cAMP than PDE4 in the rat (Harrison et al, 1986). Consequently, PDE3 plays a more significant role in regulating cAMP pools during resting conditions. As such, PDE4 activity is expected to contribute more to cAMP hydrolysis as the concentration increases, and may explain why PDE4 appears to be so dominant when inhibited during an agonist-enhanced period.

In summary, PDE4s are suspected to play such an important role because they have a great deal of molecular diversity, and have been shown to possess differential sub-cellular localization (Richter et al, 2005). However, whether particular isoforms of PDE4

are functionally coupled to certain GPCRs is still unknown, and remains to be discovered.

Experimental Limitations and Future Directions of Research

Our studies were primarily limited by the fact that we have narrowed our focus to the use of PDE3 and PDE4 inhibitors. It is possible that other families could play a role in the pathways we are exploring. Our attempts to combine the inhibition or use IBMX were unfortunately unsuccessful due to significant increases in cell shortening and calcium overload. However, in the future, alternative selective PDE inhibitors could be used to assess the effects of PDE1 and PDE2.

In addition, we have simplified our experiments to focus on the role of cAMP, and ignoring the potential contributions of cGMP. PDE3 is known to be cGMP-inhibited, which could create cross-talk effects that could confound our results. However, because we were using agonists that are known to increase cAMP, we felt that cGMP effects were minimal.

Additionally, this project focused primarily on where various PDE isoforms were functionally localized. However, two important aspects were beyond the scope of research of this project. Firstly, it would be interesting to determine whether certain specific variants of each isoform are functionally coupled with specific receptors. Furthermore, it would be interesting to investigate which scaffolding proteins are involved in creating these coupled responses, and whether these are receptor specific. In the future, we continue our efforts to develop methods to maintain cells in culture

conditions for periods sufficient to complement our pharmacological approach with a molecular approach as well, such as the use of siRNA or incubation with AKAP inhibitors like st-Ht31 (Promega). Such an approach would also be useful in determining exactly how PDE3 is localized at the sarcomere.

Our lab was also were unable to measure other components of the ECC. For instance it has been shown that Na^{+}-Ca^{2+} exchanger (NCX) and sarcolemmal Ca^{2+}-ATPase activity is promoted with PDE3 inhibition (Alousi et al, 1986, Mylotte et al, 1985). It would be interesting to see if any of these are altered when the cell is stimulated using a receptor mediated agonist.

Finally, it has been documented that PDE activity and contractile responses alter in models of disease (Reviewed in Osadchii, 2008). For instance, it has been shown that PDE3 and PDE4 increased in expression and activity in Dahl salt-sensitive rats in response to pressure-overload cardiac hypertrophy (Takahashi et al, 2002). It has also been shown that PDE inhibitors are attenuated in human heart failure and animal models (Bartel et al, 1996). Findings such as these are thought to be related to reduced myocardial concentrations of cAMP.

Thus, it is possible that compartmentation becomes disorganized in disease. Currently, there is a significant amount of debate on this topic, which is often attributed to lack of consistency in animal models. Furthermore, there is little work done in the area of how disease affects receptor specific PDE activity. Nonetheless, if dysregulation is present, it would be an important avenue to explore, since most therapeutic advances focus on targets that are altered during disease.

Final Remarks

Overall, our study assessed how PDE3 and PDE4 inhibition affected excitation-contraction coupling mechanisms when cardiac myocytes were treated with either PGE_2 or FSK. We found that various cellular parameters responded differently to PDE inhibition when treated with either agonist. When viewed in the context of the literature, our findings help to demonstrate that the location of cAMP production and degradation are indeed important in creating a compartmentalized signal. Thus, we propose that the receptor, adenylate cyclases, and PDEs are all strategically placed near their typical targets to create the unique effects associated with each distinct receptor agonist. Future research should assess how these patterns are altered during disease, and which PDE isoforms can be targeted to ameliorate contractile function without disrupting the careful organization in the cell.

REFERENCES

Akita T, Joyner RW, Lu C, Kumar R & Hartzell HC (1994) Developmental changes in modulation of calcium currents of rabbit ventricular cells by phosphodiesterase inhibitors. Circulation 90, 469-478.

Alousi AA & Johnson DC (1986) Pharmacology of the bipyridines:amrinione and milrinone. Circulation 73, 10-24.

Alta N, Soderlin SH, Hoshi N, Langeberg LK, Fayos R, Jennings PA & Scott JD (2003) Bioinformatic design of A-kinase anchoring protein-in silico: a potent and selective peptide antagonist of type II protein kinase A anchoring. Proc Natl Acad Sci USA 100, 4445-4450.

Banyasz T, Lozinskiy I, Payne CE, Edelmann S, Norton B, Chen B, Chen-Izu Y, Izu LT & Balke CW (2007) Transformation of adult rat cardiac myocytes in primary culture. Exp Physiol 93, 370-382.

Barry DM & Nerbonne J (1996) Myocardial potassium channels: Electrophysiological and molecular diversity. Annu Rev Physiol 58, 363-394.

Bartel S, Stein B, Eschenhagen T, Mende U, Neumann J, Schmitz W, Krause E, Karczewski P & Scholz H (1996) Protein phosphorylation in isolated trabeculae from nonfailing and failing human hearts. Mol Cell Biochem 157, 171-9.

Beavo J & Brunton L (2002) Cyclic nucleotide research – still expanding after half a century. Nature Sept 3, 710-718.

Bers D & Perez-Reyes (1999) Ca channels in cardiac myocytes: structure and function in Ca influx and intracellular Ca release. Cardiovasc Res 42, 339-360.

Bode D, Kanter JR & Brunton LL (1991) Cellular distribution of phosphodiesterase isoforms in rat cardiac tissue. Circ Res 68, 1070-1079.

Bos CL, Richel DJ, Ritsema T, Peppelenbosch MP & Versteeg HH (2004) Prostanoids and prostanoid receptors in signal transduction. Int J Biochem Cell Biol 36, 1187–1205.

Brodde OE (1993) Beta-adrenoceptors in cardiac disease. Pharmacol Ther 60, 405-430.

Carr D, Stofko-Hahn RE, Fraser ID, Cone RD & Scott JD (1992) Localization of the cAMP-dependent protein kinase to the postsynaptic densities by A-kinase anchoring proteins: characterization of AKAP79. J Biol Chem 24, 16816-16823.

Castro L, Verde I, Cooper D & Fischmeister R (2006) Cyclic Guanosine Monophosphate Compartmentation in Rat Cardiac Myocytes. Circulation 113, 2221-2228.

Corbin JD, Sugden P, Lincol TM & Keely SL (1997) Compartmentalization of adenosine 3’5’-monophosphate and adenosine 3’5’monophosphate-dependent kinase in heart tissue. J Biol Chem 252, 3854-3861.

Defer N, Best-Belpomme M & Hanoune J (2000) Tissue specificity and physiological relevance of various isoforms of adenylyl cyclase. Am J Physio Ren Physiol. 279, F400-F416.

Ding B, Abe J, Wei H, Huang Q, Walsh RA, Molina Ca, Zhao A, Sadoshima J, Blaxall BC, Berk B & Yan C (2005) Functional role of phosphodiestase 3 in cardiomyocyte apoptosis. Implication in heart failure. Circulation 111, 2469-2476.

Dodge-Kafka K, Langeber L & Scott JD (2006) Compartmentation of cyclic nucleotide signaling in the heart: The role of A-kinase anchoring proteins. Circ Res 98, 993-1001.

Espinasse I, Iourgenko V, Defer N, Samson F, Hanoune J & Mercadier J (1995) Type V, but not type VI, adenylyl cyclase mRNA accumulates in the rat heart during ontogenic development. Correlation with increased global adenylyl cyclase activity. J Mol Cell Cardiol 27, 1789-1795.

Fink MA, Zakhary DR, Mackey JA, Desnoyer R, Apperson-Hanse C, Damron D & Bond M (2001) AKAP-mediated targeting of protein kinase A regulates contractility in cardiac myocytes. Circ Res 88, 291-297.

Fischmeister R, Castro L, Abi-Gerges A, Rochais F & Vandecasteele G (2005) Species- and tissue-dependent effects of NO and cyclic GMP on cardiac ion channels. Comp Biochem Physio A Mol Integr Physiol 142, 136-143.

Fischmeister R, Castro L, Abi-Gerges A, Rochais F, Jurevicius J, Leroy J & Vandecasteele G (2006) Compartmentation of cyclic nucleotide signaling in the heart: the role of cyclic nucleotide phosphodiesterases. Circ Res 99, 816-828.

Frace Am, Mery P, Fischmeister R & Hartzell HC (1993) Rate-limiting steps in the beta-adrenergic stimulation of cardiac calcium current. J Gen Physiol 101, 337-353.

Gautel M, Zuffardi O, Freiburg A & Labeit S (1995) Phosphorylation switches specific for the cardiac isoform of myosin binding protein-C: a modulator of cardiac contraction?. Embo J 14, 1952-1960.

Hagemann D & Xiao RP (2002) Dual site phospholamban phosphorylation and its physiological relevance in the heart. Trends Cardiovasc Med 12, 51-56

Hambleton R, Krall J, Tikishvili E, Honeggar M, Ahmad F, Manganiello V & Movsesia MA (2005) Isoforms of PDE3 and their contribution to cAMP hydrolytic activity in subcellular fractions of human myocardium. J Biol Chem 280, 39168-39174.

Hanoune D & Defer N (2001) Regulation and role of adenylyl cyclase isoforms. Annu Rev Pharmacol Toxicol.41, 145-174.

Harrison SA, Chang ML & Beavo JA (1986) Differential inhibition of cardiac cyclic nucleotide phosphodiesterase isozymes by cardiotonic drugs. Circulation 73, 109-16.

Hayes JS, Brunton LL, Brown JH, Reese JB & Mayer SE (1976) Hormonally specific expression of cardiac protein kinase activity. Proc Natl Acad Sci USA 76, 1570-1574.

Hayes JS, Brutnon LL & Mayer SE (1980) Selective activation of particulate cAMP-dependent protein kinase by isoproterenol and prostaglandin E1. J Biol Chem 255, 5113-5119.

Hohl C & Li Q (1991) Compartmentation of cAMP in adult canine ventricular myocytes. Relation to single-cell free Ca transients. Circ Res 69, 1369-1379.

Holz G, Kan G, Harbeck M, Roe MW & Chepurny OG (2006) Cell physiology of cAMP sensor Epac. J Physiol 577, 5-15.

Houslay MD, Baillie GS & Maurice D (2007) cAMP-specific phosphodiesterase-4 enzymes in the cardiovascular system: a molecular toolbox for generating compartmentalized cAMP signaling. Circ Res 100, 950-966.

Hulme JT, TC Lin, RE Westenbroek, T Scheuer & Catterall WA (2003) B-Adrenergic regulation requires direct anchoring of PKA to cardiac Cav1.2 channels via a leucine zipper interaction with A kinase-anchoring protein 15. P Natl Acad Sci USA 100, 13093-13098.

Insel PA, Head BP, Ostrom RS, Patel H, Swaney JS, Tang CM & Roth DM (2005) Caveolae and lipid rafts: G-protein-coupled receptor signalling microdomains in cardiac myocytes.Ann N Y Acad Sci 1047, 166-172.

Jurevicius J & Fischmeister R (1996) cAMP compartmentation is responsible for a local activation of cardiac Ca channels by B-adrenergic agonists. Proc Natl Acad Sci USA 93, 295-299.

Karpen JW & Rich TC (2001) The fourth dimension in cellular signaling. Science 293, 2204-2205.

Kauffman RF, Crowe VG, Utterback BG & Robertson DW (1986) LY195115: a potent, selective inhibitor of cyclic nucleotide phosphodiesterase located in the sarcoplasmic reticulum. Mol Pharmacol 30, 609-616.

Kerfant BG, Zhao D, Lorenzen-Schmidt I, Wilson LS, Cai S, Chen SR, Maurice DH & Backx PH (2007) PI3Kgamma is required for PDE4, not PDE3, activity in subcellular microdomains containing the sarcoplasmic reticular calcium ATPase in cardiomyocytes. Circulation Research 101, 400-8.

Klein AL, Wold LE & Ren J (2004) The cyclooxygenase-2 product prostaglandin E2 modulates cardiac contractile function in adult rat ventricular cardiomyocytes. Pharmacol Res 49, 99-103.

Kithas PA, Artman M, Thompson WJ & Strada SJ (1988) Subcellular distribution of high-affinity type IV cyclic AMP phosphodiesterase activity in rabbit ventricular myocardium: relations to the effects of cardiotonic drugs. Circ Res 62, 782-9.

Kotera J, Fujishige K, Akatsuka H, Imai Y, Yanaka N & Omori K (1998) Novel alternative splice variants of cGMP-binding cGMP-specific phosphodiesterase. J Biol Chem, 273, 26982-26990.

Lehnart SE, Wehrens X, Reiken S, Warrier S, Belevych AE, Harvey RD, Richter W, Jin SL, Conti M & Marks A (2005) Phosphodiesterase 4D deficiency in the ryanodine-receptor complex promotes heart failure and arrhythmias. Cell 123, 25-35.

Lissandro V & Zaccolo M (2006) Compartmentalized cAMP/PKA signaling regulates cardiac excitation-contraction coupling. J Muscle Res Cell Motil 27, 399-403

Lugnier C, Gauthier C, Le Bec A & Soustre H (1992) Cyclic nucleotide phosphodiesterases from frog atrial fibers: isolation and drug sensitivities. Am J Physiol 262, 654-60.

Lugnier C, Muller B, Le Bec A, Beaudry C & Rousseau E (1993) Characterization of indolidan- and rolipram-sensitive cyclic nucleotide phosphodiesterases in canine and human cardiac microsomal fractions. J Pharmacol Exp Ther 265, 1142-51.

Martinez S, Beavo J & Hol WG (2002) Gaf domains: Two-billion-year-old molecular switches that bind cyclic nucleotides. Mol Intervent 2, 317-323.

Martins T, Mumby MC & Beavo J (1982) Purification and characterization of a cycli GMP-stimulated cyclic nucleotide phosphodiesterase from bovine tissues. J Biol Chem 257, 1873-1979.

Marx SO, Kurokawa J, Reiken S, Motoike H, D'Armiento J, Marks AR & Kass RS (2002) Requirement of a macromolecular signalling complex for B adrenergic receptor modulation of the KCNQ1-KCNE1 potassium channel. Science 295, 496-499.

Mendez M & LaPointe MC (2002) Trophic effects of the cyclooxygenase-2 product prostaglandin E2 in cardiac myocytes. Hypertension 39, 382-8.

Mery P, Pavoine C, Belhassen L, Pecker F & Fischmeister R (1993) Involvement of cGMP-inhibited and cGMP-stimulated phosphodiesterases through guanylyl cyclase activation. J Biol Chem 268, 26286-26295.

Meszaros J, Coutinho J, Bryant SM, Ryder KO & Hart G (1997) L-type calcium current in catecholamine-induced cardiac hypertrophy in the rat. Exp Physiol 82, 71-83.

Mongillo M, McSorley T, Evellin S, Sood A, Lissandron V, Terrin A, Huston E, Hannawacker A, Lohse M, Pozzan T, Houslay MD & Zaccolo M (2004) Fluorescence resonance energy transfer-based analysis of cAMP dynamics in live neonatal rat cardiac myocytes reveals distinct functions of compartmentalized phosphodiesterases. Circ Res 95, 67-75.

Mongillo M, Tocchetti C, Terrin A, Lissandron V, Cheung YF, Dostmann WR, Pozzan T, Kass D, Paolocci N, Houslay M & Zaccolo M (2006) Compartmentalized phosphodiesterase-2 activity blunts beta-adrenergic cardiac inotropy via an NO/cGMP-dependent pathway. Circ Res 98, 226-234.

Mongillo M & Zaccolo M (2006) A complex phosphodiesterase system controls B-adrenoceptor signaling in cardiomyocytes. Biochem Soc Trans 34(4), 510-511.

Morel E, Marcantoni A, Gastineau M, Birkedal R, Rochais F, Garnier A, Lompre AM, Vandecasteel G & Lezoualc'h F (2005) cAMP-binding protein Epac induces cardiomyocyte hypertrophy. Circ Res 97, 1296-1304.

Movsesian MA, Smith CJ, Krall J, Bristow MR & Manganiello VC (1991) Sarcoplasmic reticulum-associated cyclic adenosine 5'- monophosphate phosphodiesterase activity in normal and failing human hearts. J Clin Invest 88, 15-9.

Mylotte KM, Cody V, Davis PJ, Davis FB, Blas SD & Schoenl M (1985) Milrinone and thyroid hormone stimulate myocardial membrane Ca^{2+}-ATPase activity and share structural homologies. Proc Natl Acad Sci U S A 82, 7974-8.

Nicholson CD, Challiss RA & Shahid M (1991) Differential modulation of tissue function and therapeutic potential of selective inhibitors of cycli nucleotide phosphodiesterase isoenzymes. Trends Pharmacol Sci 12, 19-27.

Nikolaev VO, Gambaryan S, Engelhardt S, Walter U & Lohse M (2005) Real-time monitoring of the PDE2 activity of live cells: hormone-stimulated cAMP hydrolysis is faster than hormone-stimulated cAMP synthesis. J Biol Chem 280, 1716-1719.

Nikolaev VO, Bunemann M, Schmitteckhert E, Lohse MJ & Engelhardt S (2006) Cyclic AMP imaging in adult cardiac myocytes reveals far-reaching beta1-adrenergic but locally confined beta2-adrenergic receptor-mediated signaling. Circ Res 99, 1084-1091.

Okruhlicova L, Tribulova N, Styk J, Eckly A, Lugnier C & Slezak J (1997) Species differences in localization of cardiac cAMP-phosphodiesterase activity: A cytochemical study. Mol Cell Biol 173, 183-188.

Omori K & Kotera J (2007) Overview of PDEs and their regulation. Circ Res 100, 309-327.

Orchard C & Brette F (2008) T-tubules and sarcoplasmic reticulum function in cardiac ventricular myocytes. Circ Res 77, 237-244.

Osadchii OE (2007) Myocardial phosphodiesterases and regulation of cardiac contractility in health and cardiac disease. Cardiovasc Drugs Ther 21, 171-194.

Packer M, Carver JR, Rodeheffer RJ, Ivanhoe R, Dibianco R, Zeldis S, Hendrix G, Bommer WJ, Ekayam U & Kukin ML (1991) Effect of oral milrinone on mortality in severe chronic heart failure. The PROMISE study research group. N Engl J Med 325, 1468-1475.

Perrone SV & Kaplinsky EJ (2005) Calcium sensitizer agents: A new class of inotropic agents in the treatment of decompensated heart failure. Int J Cardiol 103, 248-255.

Perry SJ, Baillie G, Kohout TA, McPhee I, Magiera M, Ang KL, Miller WE, McLean AJ, Conti M, Houslay MD & Lefkowitz RJ (2002) Targeting of cyclic AMP degradation to B2-adrenergic receptors by B-Arrestins. Science 298, 834-836.

Ping PP, Anzai T, Gao M, Hammond H (1997) Adenylyl cyclase and G protein receptor kinase expression during development of heart failure. Am J Physiol Heart Circ Physiol 42, H707-H717.

Rangarajan S, Enserink J, Kuiperij HB, de Rooij J, Price LS, Schweded F & Bos JL (2003) Cyclic AMP induces integrin-mediated cell adhesion through Epac and Rap1 upon stimulation of the beta 2-adrenergic receptor. J Cell Biol 160, 487-493.

Rapundalo S, Solaro RJ & Kranias E (1989) Inotropic responses to isoproterenol and phosphodiesterase inhibitors in intact guinea pig hearts. Comparison of cyclic AMP levels and phosphorylation of sarcoplasmic reticulum and myofibrillar proteins. Circ Res 64, 104-111.

Reeves ML, Leigh BK & England PJ (1987) The identification of a new cyclic nucleotide phosphodiesterase activity in human andgu inea-pig cardiac ventricle. Biochem J 241, 535-41.

Rich TC, Fagan KA, Nakata H, Schaack J, Cooper DM & Karpen JW (2000) Cyclic nucleotide-gated channels colocalize with adenylyl cyclase in regions of restricted cAMP diffusion. J Gen Physiol 116, 147-161.

Rich TC, Fagan KA, Tse T, Schaack J, Cooper DM & Karpen JW (2001) A uniform extracellular stimulus triggers distinct cAMP signals in different compartments of a simple cell. Proc Nat Acad Sci U S A 98, 13049-13054.

Richter W, Jin SL & Conti M (2005) Splice variants of the cyclic nucleotide phosphodiesterase PDE4D are differentially expressed and regulated in rat tissue. Biochem J 388, 803-811.

Rochais F, Abi-Gerges A, Horner K, Lefebvre F, Cooper D, Conti M, Fischmeister R & Vandecasteel G (2006) A specific pattern of phosphodiesterases controls the cAMP signals generated by different Gs-Coupled receptors in adult rat ventricular myocytes. Circ Res 98, 1081-1088.

Rybin VO, Xu X, Lisanti M & Steinberg S (2000) Differential targeting of B-adrenergic receptor subtypes and adenylyl cyclase to cardiomyocyte caveolae: a mechanism to functionally regulate the cAMP signaling pathway. J Biol Chem 275, 41447-41457.

Scott JD (1993) Cyclic nucleotide-dependent protein kinases. Pharmacol Ther 139, 137-156.

Schwartz JM (2007) Compartmentation of the B-adrenergic signal by phosphodiesterases in adult rat ventricular myocytes. Unpublished Data, MSc. Thesis.

Senzaki H, Smith C, Juang GJ, Isoda T, Mayer S, Ohler A, Paolocci N, Tomaselli GF, Hare J & Kass D (2001) Cardiac phosphodiesterase 5 (cGMP-specific) modulates B-adrenergic signaling in vivo and is down-regulated in heart failure. FASEB J 15, 1718-1726.

Shah AM & MacCarthy PA (2000) Paracrine and autocrine effects of nitric oxide on myocardial function. Pharmacol Ther 86, 49-86.

Shahid M & Nicholson CD (1990) Comparison of cyclic nucleotide phosphodiesterase isoenzymes in rat and rabbit ventricular myocardium: positive inotropic and phosphodiesterase inhibitor effects of Org 30029, milrinone, and rolipram. N-S Arch Pharmacol 342, 698-705.

Shakur Y, Fong M, Hensley J, Cone J, Movsesian MA, Kambayashi JI, Yoshitake M & Liu Y (2002) Comparison of the effects of cilostazol and milrinone on cAMP-PDE activity, intracellular cAMP and calcium in the heart. Cardiovasc Drugs Ther 16, 417-27.

Smith CJ, He J, Ricketts SG, Ding J, Moggio RA & Hintze TH (1998) Downregulation of right ventricular phosphodiesterase PDE-3A mRNA and protein before the development of canine heart failure. Cell Biochem Biophys 29, 67-88.

Somekawa S, Fukuhara S, Nakaoka Y, Fujita H, Saito Y & Mochizuki N (2005) Enhanced functional gap junction neoformation by protein kinase A-dependent and Epac-dependent signals downstream of cAMP in cardiac myocytes. Circ Res 97, 655-662.

Stefan E, Wiesner B, Baillie GS, Mollajew R, Henn V, Lorenz D, Furkert J, Santamaria K, Nedvetsky P, Hundsrucker C, Beyermann M, Krause E, Pohl P, Gall I, Macintyre A, Bachmann S, Houslay MD, Rosenthal W & Klussman E (2007) Compartmentalization of cAMP-dependent signalling by phosphodiesterase-4D is involved in the regulation of vasopressin-mediated water reabsorption in renal principal cells. J Am Soc Nephrol 18, 199-212.

Strang KT, Sweitzer N, Greaser M & Moss RL (1994) Beta-adrenergic receptor stimulation increases unloaded shortening velocity of skinned single ventricular myocytes from rats. Circ Res 74, 542-549

Sugioka M, Ito M, Masuoka H, Ichikawa K, Konishi T, Tanaka T & Nakano T (1994) Identification and characterization of isozymes of cyclic nucleotide phosphodiesterases in human kidney and heart, and the effects of new cardiotonic agents on these isoenzymes. N-S Arch Pharmacol 350, 284-293.

Takahashi K, Osanai T, Nakano T, Wakui M & Okumura K (2002) Enhanced activities and gene expression of phosphodiesterase types 3 and 4 in pressure-induced congestive heart failure. Heart Vessels 16, 249-56.

Tasken J & Aandahl E (2004) Localized effects of cAMP mediated by distinct routes of protein kinase A. Physiol Rev 84, 137-167.

Terrenoire C, Houslay MD, Baillie GS & Kass RS (2009) The cardiac IKs potassium channel macromolecular complex includes the phosphodiesterase PDE4D3. J Biol Chem 284, 9140-9146.

Verde I, Pajlke G, Salanova M, Zhang G, Wang S, Coletti D, Onuffer J, Catherine Jin SL & Conti M (2001) Myomegalin is a novel protein of the golgi/centrosome that interacts with a cyclic nucleotide phosphodiesterase. J Biol Chem 276, 11189-11198.

Verde I, Vandecasteele G, Lezoualc'h F & Fischmeister R (1999) Characterization of the cyclic nucleotide phosphodiesterase subtypes involved in the regulation of the L-Type Ca^{2+} current in rat ventricular myocytes. Brit J Pharmacol 127, 65-74.

Walsh D, Perkins J & Krebs E (1968) An adenosine 3'-5'-monophosphate-dependent protein kinase from rabbit skeletal muscle. J Biol Chem 243, 3763-3765.

Weishaar RE, Kobylarz-Singer DC, Steffen RP & Kaplan HR (1987) Subclasses of cyclic AMP-specific phosphodiesterase in left ventricular muscle and their involvement in regulating myocardial contractility. Circ Res 61, 539-47.

Wheeler-Jones C. (2005) Cell signaling in the cardiovascular system: an overview. Heart 91, 1366-1374.

Xiong W, Moore HM, Howlett SE & Ferrier GR (2001) In contrast to forskolin and 3-isobutyl- 1-methylxanthine, amrinone stimulates the cardiac voltage-sensitive release mechanism without increasing calcium-induced calcium release. J Pharmacol Exp Ther 298, 954-63.

Zaccolo M (2006) Phosphodiesterases and compartmentalized cAMP signaling in the heart. Eur J Cell Biol 85, 693-697.

Zaccolo M & Movsesian M (2007) cAMP and cGMP signaling cross-talk: role of phosphodiesterases and implications for cardiac pathophysiology. Circ Res 100, 1569-1578.

Zaccolo M & Pozzan T (2002) Discrete microdomains with high concentration of cAMP in stimulated rat neonatal cardiac myocytes. Science 295, 1711-1715.